Removal of Vancomycin from Water by adsorption using waste materials

Northern Ireland Biomedical Engineering Society

Annual Symposium 2023

Wednesday 5th April

Programme

Contents

Sponsors

The organising committee would like to thank Ashland and Merck for their kind sponsorship and support for the NIBES 23 annual symposium:

https://www.ashland.com/

Merck | United Kingdom | Life Science Products & Service Solutions (sigmaaldrich.com)

Welcome from NIBES President

It is with great pleasure that I welcome you to the annual Northern Ireland Biomedical Engineering Symposium hosted by Queen's University Belfast. The Northern Ireland Biomedical Engineering Society is dedicated to encouraging and developing collaborative links between research teams, universities, industry, and clinicians. The past number of years have been challenging for us all, but it is wonderful to see so many colleagues and collaborators from across Northern Ireland able to gather to network and discuss research in a face-to-face setting again. We have received a large volume of high-quality abstracts, so today promises to be an excellent day of science and discussion and I hope that you use this opportunity today to chat, network and initiate fruitful collaborations.

This year at the symposium we are excited to have a public vote on our new society logo, thank you very much to all the excellent submissions, we are also excited to formally launch the NIBES website (sites.google.com/view/nibes), this site will be used to share up to date information about upcoming events and competitions as well as hold a record of the previously held symposia and programmes.

I would like to take this opportunity to thank our sponsors for today's symposium: Ashland and Merck, their support has allowed us to run today's event in-person and provide a light lunch. I would also like to thank the various members of the NIBES committee for their continual support and efforts in organising the symposium.

Kind Regards,

Dr Jonathan Acheson,
Lecturer, School of Engineering
President of NIBES
Ulster University

Committee

https://sites.google.com/view/nibes/committee

Conference Programme

09:00 – 09:05	**Arrival**	
09:05 – 09:10	**Welcome**	*Jonathan Acheson*
09:10 – 11:30	**Session 1**	Chairs: *Pamela Walsh, Robyn Macartney*

09:10 – 09:30 **Keynote: Susan Clarke QUB**

09:30 – 09:40 **Shuai Zhang, QUB**
INFLUENCE OF FIBRINOGEN DEPOSITION ON ANTIFOULING PROPERTY OF SILICON OIL-INFUSED URINARY CATHETERS

09:40 – 09:50 **Hamed Rasouli Sadabad, UU**
EFFECT OF ACTIVATED CARBON CHARACTERISTICS ON ITS ABILITY TO REMOVE VANCOMYCIN AND RIFAMPICIN FROM WATER

09:50 – 10:00 **Tiancheng Luo, QUB**
ANTIBACTERIAL AND ANTI-ENCRUSTATION WEAK ORGANIC ACIDS- LOADED PLA COATING ON URINARY CATHETERS

10:00 – 10:10 **Jude Cameron, QUB**
COMPARING MEDICAL AND PACKAGING GRADE PLLA FOR BIORESORBABLE VASCULAR SCAFFOLD APPLICATIONS

10:10 – 10:20 **Yidan Luo, QUB**
DEVELOPMENT OF ANTIVIRAL LOADED MICRONEEDLE DELIVERY SYSTEMS FOR HEPATITIS B TREATMENT

10:20 – 10:30 **Charlie Bateman, QUB**
SYNTHESIS AND CHARACTERISATION OF NOVEL BIOPOLYMERS FOR LIGAMENT TISSUE ENGINEERING

10:30 – 10:40 **Jiawen Wang, QUB**
DEVELOPMENT OF ANTI-LEISHMANIASIS DRUG AMPHOTERICIN B NANOCRYSTAL-BASED DISSOLVING MICRONEEDLE FOR INTRADERMAL DELIVERY

10:40 – 10:50 **Aoife McFerran, UU**
DUAL FUNCTIONAL LBL ASSEMBLY NANOCOMPOSITE COATINGS FOR MECHANICAL REINFORCEMENT OF BONE TISSUE SCAFFOLDS AND ENHANCEMENT OF BONE DEFECR REPARATION VIA INCORPORATION OF THERAPEUTIC AGENTS.

10:50 – 11:00 **Robyn Irwin, QUB**
A BRIGHT FUTURE: PHOTODYNAMIC ANTIMICROBIAL POLYMER FILMS WITH POTENTIAL USE AS ENDOTRACHEAL TUBE COATINGS FOR THE PREVENTION OF VENTILATOR ASSOCIATED PNEUMONIA

11:00 – 11:10 **Samuel Tiplady, QUB**
MANUFACTURING AND CHARACTERISATION OF A 3D PRINTED POLYMER/CERAMIC SCAFFOLD FOR THE REPAIR AND REGENERATION OF CRITICAL-SIZED BONE DEFECTS

11:10 – 11:20 **Jingyi Xu, QUB**
DEVELOPMENT OF ANTIBACTERIAL URINARY CATHETER FOR PH RESPONSIVE HYDROGEL COATINGS RELEASED RIFAMPICIN

11:20 – 11:30 **Dan Sun, QUB**
MULTIFUNCTIONAL NANOCOMPOSITES FOR BONE IMPLANT APPLICATIONS

11:30 – 12:30	**PhD Training/Speed Networking Event**	
12:30 – 13:15	**Lunch**	
13:15 – 15:25	**Session 2**	Chairs: *Joanna Ward, Aoife McFerran*
13:15 – 13:35	**Keynote: Ryan Donnelly, QUB**	

RAPID FIRE PRESENTATIONS

13:35 – 13:40 **Jacob Jenson, UU**
COMPUTATIONAL EVALUATION OF SKULL AND SPRING PARAMETERS IN SPRING ASSISTED SAGITAL SYNOSTOSIS CORRECTION

13:40 – 13:45 **Jasmine Ross, QUB**
BIOMATERIAL COATINGS WITH LUBRICIOUS, SLIPPERY PROPERTIES FOR IMPROVED URINARY CATHETER PERFORMANCE

13:45 – 13:50 **Frances Hasson, UU**
PEKK-HYDROXYAPATITE COMPOSITES FOR PATIENT MATCHED 3D PRINTED MEDICAL IMPLANTS

13:50 – 13:55 **Ruolan Chen, QUB**
ENHANCED ANTI-BIOFILM AND ANTI-PROTEIN ADSORPTION PROPERTIES OF LIQUID-INFUSED SILVER-POLYTETRAFLUOROETHYLENE COATINGS

13:55 – 14:00 **Eimear O'Donnell, UU**
MODELLING THE PROPERTIES OF 3D PRINTED PARTS MADE WITH ADVANCED MATERIALS

14:00 – 14:05 **Elizabeth Magill, QUB**
IMPLANTABLE DEVICES FOR CANCER TREATMENT

14:05 – 14:10 **Reshma McMullan, UU**
3D PRINTING OF PEEK APATITE COMPOSITES FOR ORTHOPEADIC IMPLANTS

14:10 – 14:15 **Camila Picco, QUB**
DEVELOPMENT OF 3D PRINTED SUBCUTANEOUS IMPLANTS USING CONCENTRATED POLYMER/DRUG SOLUTIONS

14:15 – 14:20 **Kaifeng Huang, QUB**
MODULATION OF BACTERIAL INFECTION AND INFLAMMATION BY A LACTIDE-LOADED MATRIX SYSTEM

14:20 – 14:25 **Martina Sangalli, UU**
PRODUCTION OF GEL PATCHES LOADED WITH ACYCLOVIR NANOCRYSTALS

FULL PRESENTATIONS

14:25 – 14:35 **Oscar Denton, QUB**
ROBUST ALGORITHM FOR DENSE SHAPE CORRESPONDENCE

14:35 – 14:45 **Junting Yao, QUB**
CONJUGATION OF CATIONIC CELL PENETRATING PEPTIDE WITH NOVEL KUNITZIN-LIKE TRYPSIN INHIBITOR: NEW INSIGHTS FOR ENHANCING BIOACTIVITIES

14:45 – 14:55 **Robyn Macartney, UU**
AMOXICILLIN-LOADED PLCL ELECTROSPUN SCAFFOLDS FOR APPLICATIONS IN PERIODONTAL TISSUE ENGINEERING

14:55 – 15:05 **Prasannavenkadesan Varatharajan, QUB**
OSTEONECROSIS IN ORTHOPAEDIC DRILLING

15:05 – 15:15 **Anna Korelidou, QUB**
3D-PRINTED RESERVOIR-TYPE IMPLANTS FOR CURCUMIN DELIVERY

15:15 – 15:25 **Abudu Lekan Seun, UoL/UU**
REMOVAL OF VANOMYCIN FROM WATER BY ADSORPTION USING WASTE MATERIALS

15:25 – 15:40	**Tea Break + Vote for Logo**	
15:40 – 16:50	**Session 3**	Chairs: *Jonathan Acheson, Jude Cameron*

15:40 – 15:50 **Jane Burns, QUB**
DUAL ACTION HYDROGEL COATINGS FOR THE PREVENTION OF URINARY CATHETER INFECTIONS AND BLOCKAGES

15:50 – 16:00 **Rania Mahafdeh, QUB**
ANTIBACTERIAL ASSESSMENT OF TMPyP-INCORPORATED p(HEMA-co-MMA)

16:00 – 16:10 **Anushree Ghosh Dastidar, QUB**
INVESTIGATING THE REGENERATIVE POTENTIAL OF 3D-PRINTED PLLGA/ALGINATE COMPOSITE SCAFFOLDS FOR THE TREATMENT OF ARTICULAR CARTILAGE DEFECTS

16:10 – 16:20 **Jordan Barr, QUB**
REPLICATION OF POLYMERIC BIROESORBABLE VASCULAR SCAFFOLD PROCESSING HISTORY WITH FOCUS ON CRIMPING

16:20 – 16:30 **Humera Sarwar, UU**
ADVANCING SURGICAL CARE: BIACTIVE GLASS SYSTEM FOR TARGETED ANTIBIOTIC DELIVERY IN PREVENTION AND TREATMENT OF SURGICAL SITE INFECTIONS

16:30 – 16:40 **Alex Haskins, QUB**
DETERMINING ACTIVE DRAG IN SWIMMING VIA COMPUTATIONAL AND EXPERIMENTAL MEANS

16:40 – 16:50 **Adelaide Mensah, UU**
SYNTHESIS AND CHARACTERISATION OF SILVER NANOPARTICLES AS A COMPONENT OF ANTIBACTERIAL HYDROGEL COATINGS IN PERIODONTAL DISEASE DIAGNOSTICS

16:50 – 17:05	**Tea Break**
17:05 – 17:15	**Conference Awards and Close**

Keynote: Dr Susan Clarke, Queen's University Belfast

Susan Clarke obtained her PhD at the Interdisciplinary Research Centre in Biomedical Materials, Queen Mary and Westfield College, London and has been a biomedical scientist involved in orthopaedic research for over twenty years, with postdoctoral positions at the Orthopaedic Research Unit, University of Cambridge and Dept. of Trauma and Orthopaedic Surgery, Queen's University Belfast.

She is currently a Reader in Applied Life Science in the School of Nursing and Midwifery at Queen's University, Belfast. Her research interests lie in the area of regenerative medicine specifically looking at the development of smart biomaterials to support bone repair in a patient and application specific manner.

In addition to investigating the patient predictors of adult stem cell response in bone repair, she also works collaboratively with colleagues in School of Mechanical and Aerospace Engineering and the School of Chemistry and Chemical engineering to understand the *in vitro* and *in vivo* response to novel biomaterials and novel bioactives derived from marine organisms that can support new bone formation.

Keynote: Professor Ryan Donnelly, Queen's University Belfast

Ryan Donnelly graduated with a BSc (1st Class) in Pharmacy from Queen's University Belfast in 1999. Following a year of Pre-Registration training spent in Community Pharmacy, he returned to the School of Pharmacy to undertake a PhD in Pharmaceutics. He graduated in 2003 and, after a short period of post-doctoral research, was appointed to a Lectureship in Pharmaceutics in January 2004. He was promoted to Senior Lecturer in 2009, Reader in 2011 and, in 2013, to a Chair in Pharmaceutical Technology.

Professor Donnelly's research is centred on design and physicochemical characterisation of advanced polymeric drug delivery systems for transdermal and topical drug delivery, with a strong emphasis on improving therapeutic outcomes for patients. His bioadhesive patch design was used in successful photodynamic therapy of over 100 patients with neoplastic and dysplastic gynaecological conditions and the patent subsequently out-licensed.

He has authored over 600 peer-reviewed publications, including several granted patents, 6 textbooks and approximately 260 full papers. He has been an invited speaker at numerous national and international conferences. Professor Donnelly is the Europe/Africa Editor of Drug Delivery & Translational Research and a member of the Editorial Advisory Boards of Journal of Controlled Release, Micromachines and Expert Review of Medical Devices and is a Visiting Scientist at the Norwegian Institute for Cancer Research, where he is an Associate Member of the Radiation Biology Group. He is a Board Member of the Academy of Pharmaceutical Sciences and the Communications Chair of the Controlled Release Society. His work has attracted numerous awards, including the Academy of Pharmaceutical Sciences Innovative Science Award in 2020, the Controlled Release Society Young Investigator Award in 2016, BBSRC Innovator of the Year in 2013, the GSK Emerging Scientist Award in 2012 and the Royal Pharmaceutical Society Science Award in 2011.

Prizes

There will be a first place and second place award for oral presentations. Winners will be chosen by the committee; they will gather during the final tea/coffee break and announce the winners at the close of the symposium.

The following criteria will be used for the decision making:

- Scientific content
- Originality of research
- Use of visual aids
- Presentation style/delivery
- Presentation layout/structure

Abstracts

INFLUENCE OF FIBRINOGEN DEPOSITION ON ANTIFOULING PROPERTY OF SILICON OIL-INFUSED URINARY CATHETERS

Zhang, S.

[1] School of Pharmacy, Queen's University Belfast, Northern Ireland, BT9 7BL, UK

e-mail: shuai.zhang@qub.ac.uk

INTRODUCTION

Benefiting from the ultralow low hysteresis and slippery behaviours, slippery silicone-oil-infused (SOI) coatings have been found to effectively reduce bacterial adhesion under both static and flow conditions. However, in real clinical settings, the use of catheters (e.g., silicone, Si) may trigger local inflammation, leading to release of host-secreted proteins, fibrinogen (Fgn) that deposit on the catheter surfaces, creating a niche that can be exploited by uropathogens to cause infections [1]. In this work, we report on the fabrication of an SOI silver-releasing (AgO) catheter which was expected to prevent or retard the formation of catheter-associated biofilm and encrustation.

MATERIALS AND METHODS

The AgO urinary catheters were fabricated via a two-step method [2]. The surface morphology, chemical composition, coating thickness, contact angle hysteresis (CAH), and silver release were characterised by SEM, AFM, EDX, FTIR, ellipsometry, contact angle measurement and ICP-MS. Their durability in PBS was assessed for up to 7 days at 37 °C. Protein adsorption on coatings was determined by BCA method [3]. Their antibiofilm properties were assessed against *E. coli* and *P. mirabilis* and compared in the presence of Fgn. The effects of Fgn deposition on migration of *P. mirabilis* and encrustation in artificial urine were assessed using a bridge model and an *in vitro* encrustation model, respectively.

RESULTS

The AgO surfaces were hydrophobic (CA of 95.5° ± 1.0°) and extreme water repellent (CAH ~1.6° (Fig 1a). Upon contact with Fgn, the CAH increased on all the surfaces, despite the AgO surfaces still retaining greater repellency. The dynamic water and Fgn CAs on the surfaces of AgO slightly increased due to oil loss after 7 days' flush in water, but the AgO surfaces maintained significant stability (Figs 1b and 1c). The AgO surfaces showed significantly higher levels of Fgn binding (Fig. 1d) due to conformational change of the protein (Figs 1e and 1f) upon contact with silicone oil. Regardless of oil thickness, the absorbed Fgn facilitated biofilm formation and blocked the interaction of silver with the bacteria, resulting in an increased biofilm coverage (Figs 1g and 1h). Moreover, the surface binding with Fgn accelerated the spread of crystalline biofilm over catheter surfaces (Figs.1i, 1j and 1k).

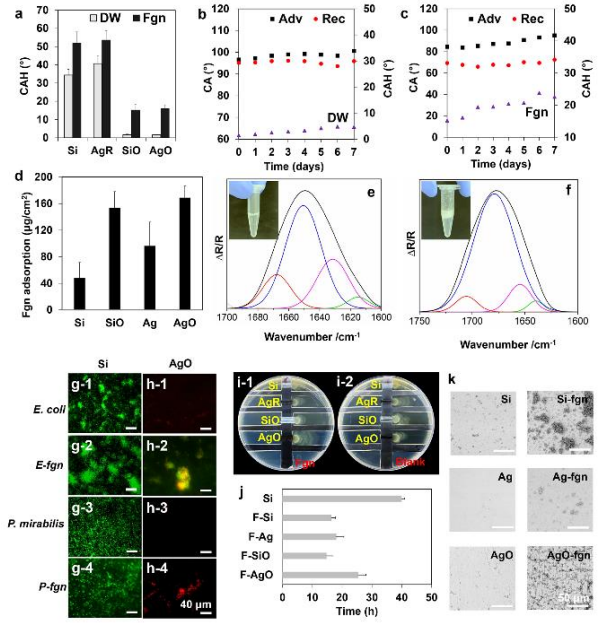

Figure 1 (a)-(c) CAH; (d) Fgn adsorption; FTIR spectra of (e) Fgn and (f) SiO-Fgn; biofilm formation on (g) Si and (h) AgO; P. mirabilis migration (i) and passage time; (k) encrustation on different samples.

DISCUSSION

The AgO catheters demonstrated superior durability due to inherent self-healing properties and outstanding antifouling properties due to water repellence. In the presence of Fgn, the AgO surface could trigger protein conformation and accelerate protein binding, which, in turn, resulted in a loss of liquid repellence and enhanced bacterial binding, migration, biofilm formation, and encrustation.

CONCLUSION

A SOI catheter may not hold significant potential for resisting infections unless catheter-associated bladder inflammation could be effectively avoided.

REFERENCES

[1] Flores-Mireles (et al.), J Urol 196: 416-421, 2016.

[2] Zhang (et al.), Langmuir 39: 1562-1572, 2023.

[3] Wei (et al.), ACS Appl Mater Interfaces 8: 34810- 34819, 2016.

EFFECT OF ACTIVATED CARBON CHARACTERISTICS ON ITS ABILITY TO REMOVE VANCOMYCIN AND RIFAMPICIN FROM WATER

Rasouli Sadabad, H.[1], Coleman, H.[2], Dooley, J.[3], Snelling, W.[3], O'Hagan, B[3], Arnscheidt, J[1]

[1] School of Geography and Environmental Sciences, Ulster University
[2] School of Pharmacy and Pharmaceutical Sciences, Ulster University
[3] School of Biomedical Sciences, Ulster University
email: rasouli_sadabad-h@ulster.ac.uk

INTRODUCTION

Presence of antibiotics in lower amounts than their minimum inhibition concentration (MIC) may impose a selection pressure on microorganisms and cause dissemination of antimicrobial resistance in aqueous environment (Matviichuk et. al, 2023). According to activated carbon's exclusive characteristics, especially its ability to adsorb various pharmaceuticals from water, it is the most frequently utilized absorbent, worldwide (Huang et al., 2022). Based on the source and activation method, activated carbons may possess different properties, and it is critical to select the appropriate adsorbent for removal of specific contaminant. This study has investigated the elimination of antibiotics vancomycin and rifampicin by two different granular activated carbons from water.

MATERIALS AND METHODS

Surface morphology, pore-characteristics, and chemical properties of the adsorbents were determined by SEM, BET, FTIR spectroscopy and Boehm titration. Concentrations of vancomycin and rifampicin were analysed by HPLC. Adsorption of antibiotics was investigated in a variety of operational conditions.

RESULTS AND DISCUSSION

Studied activated carbons were able to remove vancomycin and rifampicin from water. Observed differences in removal efficiency appeared to be related to dissimilarity in morphological properties (figure 1), e.g. there were significant positive correlations between mesopore content of the adsorbent and its effectiveness in removing antibiotics from water. Figure 2 shows that across the studied range of antibiotic concentrations, both adsorbents' removal of rifampicin exceeded that of vancomycin. Rifampicin has a higher octanol/water coefficient and a smaller molecule than vancomycin. Both of these properties would facilitate antibiotic adsorption onto the surface of activated carbon and subsequent diffusion into its porous structure. In comparison between carbons Filtrasorb-400 has a higher mesopore content and also a larger average pore size in this category. In consequence it adsorbed more of the larger sized molecule vancomycin than Norit-PK1-3, particularly at lower antibiotic concentrations.

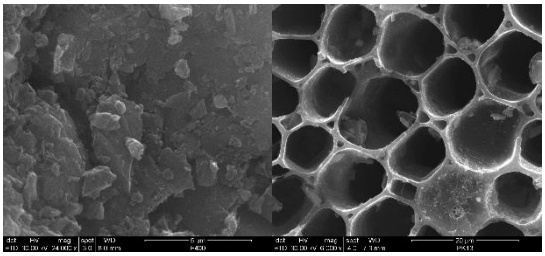

Figure 1. SEM micrographs of studied activated carbons (left: Filtrasorb-400, right: Norit-PK1-3) (Rasouli Sadabad et. al., 2022)

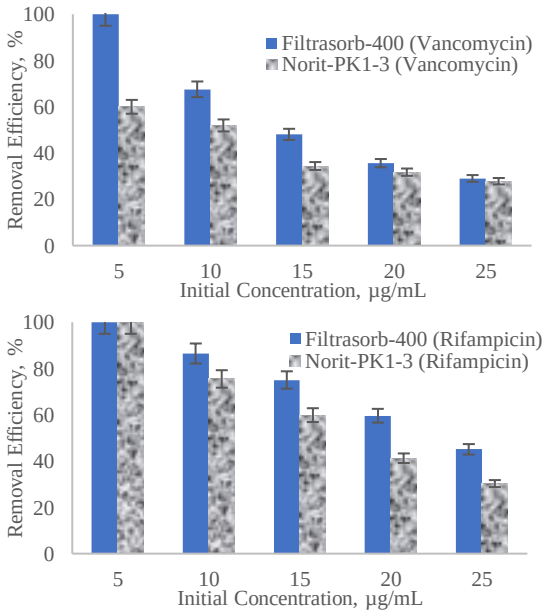

Figure 2. Removal efficiency of adsorption process vs. initial concentration

CONCLUSION

Adsorption of vancomycin and rifampicin from water by activated carbon is mainly controlled by pore diffusion. Hence, surface attributes of the adsorbent, especially pore-characteristics, play an important role in the removal of the investigated antibiotics from an aqueous environment.

REFERENCES

Huang *(et al.)*, Applied Thermal Engineering 214: 118775, 2022.
Matviichuk *(et al.)*, Water Research 231:119611, 2023.
Rasouli Sadabad *(et al.)*, 32nd Irish Environmental Researchers Colloquium, Belfast, UK, 2022

ANTIBACTERIAL AND ANTI-ENCRUSTATION WEAK ORGANIC ACIDS-LOADED PLA COATING ON URINARY CATHETERS

Tiancheng, Luo., Matthew, Wylie., Colin, McCoy.
School of Pharmacy, Queen's University Belfast
email: c.mccoy@qub.ac.uk

INTRODUCTION

As the most common device-related bacterial infections, the mortality and morbidity of catheter-associated urinary tract infections (CAUTIs) have increased significantly in recent years. (1) The complications of CAUTIs are debilitating, and include fever, difficulty in urination and kidney damage. (2)

Moreover, infected urine with elevated pH can develop urinary crystals, that can eventually block catheter eyelets, preventing drainage from the bladder. (3)

This project aims to develop a weak organic acid (WOA)-loaded polylactic acid (PLA) coating onto urinary catheters via a dip coating technique, which can not only kill bacteria by slowly releasing WOAs, but also reduce pH of urine and therefore address the problem of crystallisation.

METHODS

Firstly, WOA-loaded PLA coatings on silicone rubber substrates were prepared by dip coating. The release of WOAs from PLA polymer coatings with time was characterised.

Then, the microbiological performance was evaluated through determination of minimum inhibitory concentrations (MICs) and minimum bactericidal concentrations (MBCs), and carrying out a 2D checkboard assay, anti-adherence test and static anti-encrustation assay.

RESULTS

As **Figure 1** shows, drug release characterisation revealed that the two WOAs were completely released from PLA coatings after 3 to 8 days at pH 5.9 and 9.5, which represent pH of normal and infected urine, respectively.

Additionally, the MICs/ MBCs of lactic acid and citric acid against *P. mirabilis* (ATCC 51286） were 3/3 and 1.5/6. (mg/ mL) 2D checkboard assay showed the Fractional Inhibitory Concentration Index of the two WOAs against *P. mirabilis* was 0.375, which indicates a synergistic relationship.

Moreover, there was a >98% reduction in bacterial viability on WOA-loaded PLA coated samples compared with untreated substrates after 24h, and the crystallisation was inhibited. (**Figure 2**)

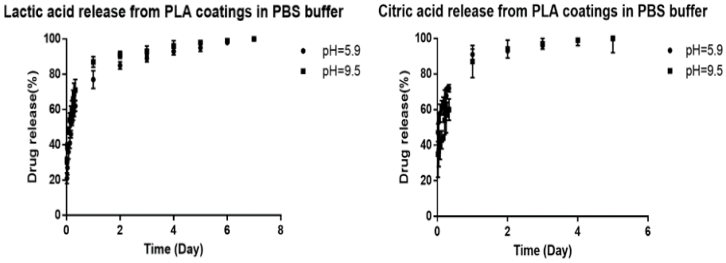

Figure 1. *Release of lactic acid and citric acid from PLA coatings in PBS at pH 5.9 and 9.5.*

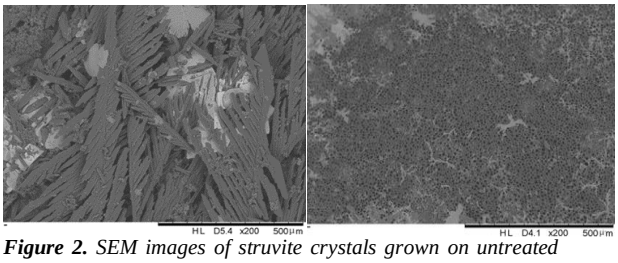

Figure 2. *SEM images of struvite crystals grown on untreated silicone rubber substrates（left）and 5% lactic acid/ 5% citric acid loaded PLA coatings (right) over 24 hours.*

CONCLUSION

In conclusion, WOAs with bactericidal activity were slowly released from PLA coatings produced by a dip coating technique. The polymer coating not only very significantly reduced bacterial adhesion onto surfaces of catheters and reduced also crystallisaion.

REFERENCES

1. Megan *(et al.)*, Critical Care Nurse Vol 40, No. 1, 2020.
2. Sawsan *(et al.)*, Journal of Microbiology Research, 10(1): 1-5, 2020.
3. Das *(et al.)*, Biomed Pharmacother. 96:361-370, 2017.

COMPARING MEDICAL AND PACKAGING GRADE PLLA FOR BIORESORBABLE VASCULAR SCAFFOLD APPLICATIONS

Cameron, J., Barr, J., Menary, G., Lennon, A.
[1] Queen's University Belfast
email: jcameron07@qub.ac.uk

INTRODUCTION

Cardiovascular diseases are the primary cause of death globally [1]. Bioresorbable vascular scaffolds (BVSs) were developed to overcome the limitations of permanent metallic stents. Poly-(l-lactic acid)(PLLA) is the preferred material choice but, with a tensile modulus lower than metal, the polymeric stents need to be ~2x as thick to achieve similar structural stiffness, hindering deployment and disrupting blood flow [2, 3].

Initially uniform PLLA is subjected to a series of thermo-mechanical processes to create a BVS, with properties strongly dependent on the thermal and strain histories experienced by the polymer — in particular, the crimping and expansion stages. There is a lack of consensus on the impact of crimping on the mechanical properties of the BVS [4]. U-bends have been highlighted as an area of interest and microcracks that form during crimping can indicate possible failure sites [5]. Crimping is thus key to creating a thinner scaffold.

Due to the cost of medical grade PLLA, it is far more feasible to carry out initial testing on a cheaper, packaging grade PLLA with a different molecular weight. This research aims to determine if the materials behave similarly enough during each phase of BVS processing for this to be a valid exercise.

MATERIALS AND METHODS

PLLA (PL38 and Luminy L175, Corbion, The Netherlands) have been extruded to a 1mm thick sheet and, using a custom biaxial stretching device [6], stretched specimens were prepared using different stretch ratios, speeds, and temperatures. Thus replicated, in a controlled manner, the range of thermal and strain history conditions the material would experience during the expansion phase of BVS manufacture.

From these biaxially stretched samples, tensile dog bones were cut using a die cutter while U-bend shaped specimens were laser cut. The tensile specimens were used for a design of experiments (DOE) study to compare the mechanical properties of the two grades of PLLA and contrast with the work of Blair et al [7] on a different grade of packaging PLLA from the same supplier. The U-bends have been used for crimp and expansion tests using a custom-built crimp rig (Fig. 1a) and x-ray diffraction experiments have been carried out on the U-bends pre- and post- crimp and expand. The microfocus beam available at beamline I22 (Diamond Light Source, Harwell, UK) was used to complete wide-angle x-ray scattering (WAXS) and small-angle x-ray scattering (SAXS) ex-situ (Fig. 1b) and in-situ experiments are pending. Data was collected with a Pilatus P3-2M detector and reduced using DAWN software. Due to the significance of molecular weight on degradation and mechanical response of PLLA, samples have been taken at each stage for gel permeation chromatography (GPC).

RESULTS AND DISCUSSION

Tensile data shows that the mechanical properties vary with stretch ratio similarly between the two materials. DoE shows stretch ratio as the dominant factor in packaging grade PLLA, as found by Blair al [7](Fig. 1e), and in medical grade PLLA (Fig. 1f). XRD shows higher percentage crystallinity for the packaging grade material (Fig. 1d). DSC showed two new peaks (endothermic followed by exothermic), hypothesised to be due to enthalpic relaxation of highly oriented amorphous chains (Fig 1c). The varying strain in the machine and transverse directions of the biaxial stretching process is expected to determine the crystallinity and crystal orientation of the U-bends. We anticipate a microstructural reorientation to occur during the crimping process that depends on the crimping conditions – namely, temperature and rate.

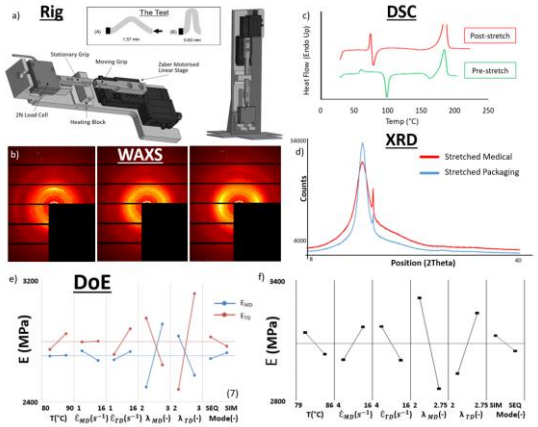

Figure 1 a) Custom-built crimp rig, b) Ex-situ WAXS diffraction patterns, c) DSC for unstretched and stretched material, d) XRD data for stretched medical and packaging grade PLLA, e) DoE main effects plot for modulus of packaging PLLA from [7], f) DoE main effects plot of medical PLLA

Packaging grade PLLA has historically been used in research relating to BVS. We have shown that for modulus and strain at break data both materials respond similarly to different processing conditions, but we anticipate the differences to lie at the microstructural level, with the semi-crystalline morphology and the orientation of the amorphous chains and crystals.

REFERENCES

[1] .who.int/news-room/fact- sheets/detail/cardiovascular-diseases-(cvds), 16/11/11 [2] Ang, H. Y. et al., Scientific Reports 8,2018. [3] Tammaro, L. et al. AIP Conference Proceedings vol. 1981, 2018 [4] Ramachandran, K. et al. Proceedings of the National Academy of Sciences of the United States of America 115, 10239–10244 (2018) [5] Wang, P. J et al.: Proceedings of the National Academy of Sciences of the United States of America 115, 2640–2645 (2018) [6] Martin, P. J et al.: Plastics, Rubber and Composites. 34, 276-282, 2005. [7] Blair et al,: Journal of Mechanical Behaviour of Biomedical Materials 97 (2019)

DEVELOPMENT OF ANTIVIRAL LOADED MICRONEEDLE DELIVERY SYSTEMS FOR HEPATITIS B TREATMENT

Luo, Y, Vora, L. K, Li, Y, Paredes, A. J, Donnelly, R.F

School of Pharmacy, Queen's University Belfast, Medical Biology Centre, 97 Lisburn Road, Belfast BT9 7BL, UK

email: R.Donnelly@qub.ac.uk

INTRODUCTION

Hepatitis B virus (HBV) infection is a major global health issue, causing nearly 1 million deaths from liver diseases yearly.[1] One of the first-line agents for HBV treatment, entecavir (ETV), is required to be taken daily under fasted state. However, this regime will undoubtedly cause inconvenience to patients, which may ultimately affect the effectiveness of the treatment.[2] As a parenteral drug delivery system, microneedles (MN) could help avoid the influence of food, as well as offer a strategy to achieve sustained drug delivery *via* the transdermal route.[3] The study aims to develop an MN system loaded with ETV, which can lead to transdermal drug delivery with sustained pharmacokinetic profiles. This study could potentially provide proof of concept that the utilisation of the MN system may offer an elegant strategy to achieve transdermal delivery of antiviral drugs such as ETV.

METHODS

To fabricate the ETV-loaded bilayer MNs, aqueous solutions of PVP-PVA (PVA, 9–10 kDa)/(PVP, 58 kDa) (20%: 20%, w/w) encapsulating ETV were cast into the MN moulds(600 pyramidal needles on a 0.76 cm^2 area with 750 µm needle height) by subjecting to a positive pressure of 5 bar. After drying overnight, drug-free polymer solution was added and centrifuged at 3500 rpm for 10 min, and then this was left at room temperature to dry. The MN patches fabricated were observed using a stereomicroscope. The *in vitro* permeation study was operated using Franz cells with full-thickness neonatal porcine skin. The drug content of the MN patches was quantified *via* a validated HPLC.

RESULTS AND DISCUSSION

Figure 1 shows the morphology of MNs patches fabricated in this study. PVA and PVP were selected as these polymers are biocompatible and have been widely used in fabricating dissolving MNs.

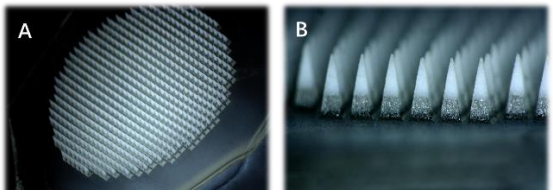

Figure 1. (a) and (b) Optical micrograph of ETV-loaded MN (30% MNs) prepared from aqueous blends of ETV (30% w/w of ETV, 6.45% w/w PVA, 6.45% w/w PVP).

Figure 2 shows the *in vitro* permeation profiles of three ETV-loaded MNs with different optimised formulations and one needle-free ETV-loaded patches in full-thickness porcine skin. The amount of drug permeation from one MN patch could achieve 1.5mg at the 24th hour after starting the *in vitro* permeation study. As the daily dosage of ETV is relatively low, necessitating only 0.5-1.0 mg per daily oral dose. Thus, the drug content in the MNs fabricated in the current work would suffice for daily oral dose of ETV.

From Figure 2(b), it can be found that most drug permeated into receptors while it was barely detected in the skin deposition as ETV is relatively hydrophilic, which shows that ETV-loaded dissolving MNs could hardly achieve long-acting drug delivery. In the future, we will focus on this limitation.

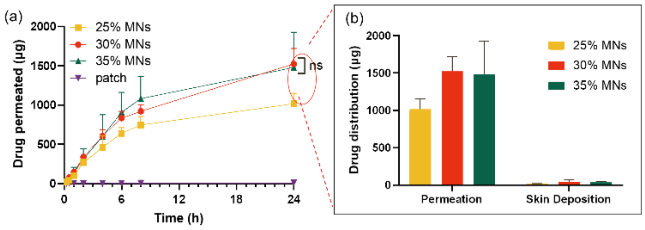

Figure 2. *(a) In vitro permeation profiles of three ETV-loaded MNs with different formulations and one needle-free ETV-loaded patches in full-thickness porcine skin. (means +S.D., n = 5; ns: p > 0.05) (b) Comparison of the amount of drug permeated into receptors and the amount of drug deposited in full-thickness porcine skin at the 24th hour after starting the in vitro permeation study. (means +S.D., n=4)*

CONCLUSION

Overall, the successful construction of ETV-loaded dissolving MNs have provided a promising approach for HBV treatment, with potential for enhanced patient compliance. It could potentially provide a proof of concept that illustrate the utilisation of MN-based system as an elegant strategy to achieve transdermal delivery of antiviral drugs. Forthcoming study could be related to delivering ETV *via* hydrogel-forming MNs to achieve long-acting drug delivery.

REFERENCES

Schweitzer *(et al.)*, Lancet, 386: 1546-1555, 2015.
Sims *(et al.)*, Pharmacotherapy, 26: 1745-1757, 2006
Tekko *(et al.)*, Adv. Funct. Mater., 32, 2022.

SYNTHESIS AND CHARACTERISATION OF NOVEL BIOPOLYMERS FOR LIGAMENT TISSUE ENGINEERING

Bateman, C., Chen, B.
Queen's University Belfast, Belfast, United Kingdom
Email:cbateman03@qub.ac.uk

INTRODUCTION

Tissue engineering is an attractive strategy for the reconstruction of ligaments. Previous work on ligament tissue scaffolds has struggled to replicate the required mechanical properties of ligament tissue for optimal tissue regeneration.

This research aims to prepare a new biopolymer which can mimic the mechanical properties of ligament tissue for potential application in ligament tissue engineering.

MATERIALS AND METHODS

Thermoplastic polyurethanes (TPUs) are a suitable candidate for this application due to the ability to modify its chemical structure and so properties.

Polycaprolactone diol, polyethylene glycol and l-lysine diisocyanate (LDI) were used in the synthesis of the new TPU. LDI degrades into non-toxic products making it better suited to the application than the typical aromatic isocyanates used. The composition of the TPU was kept constant and the reaction time was varied to achieve TPUs with target properties. No solvents or catalysts were used in the synthesis.

Samples were characterised using Fourier transform infrared spectroscopy (FTIR), nuclear magnetic resonance (NMR), gel permeation chromatography (GPC), differential scanning calorimetry (DSC), quasi-static and cyclic tensile tests, as well as biodegradation tests.

TPU scaffolds were produced by lyophilisation with a custom-made mould. Scanning electron microscopy (SEM) was used to characterise the porous structure.

RESULTS AND DISCUSSION

FITR and NMR confirm the formation of TPUs, and no residue of isocyanate functional groups in the resulting polymers. GPC gives average molecular weights of each TPU. The TPUs have a −55 °C glass transition temperature as seen on DSC and are in the rubbery state at room temperature.

The tensile strength of the dry TPUs is between 5.9 – 6.0 MPa and strain at break between 50 – 290%. A TPU swollen in a phosphate buffered saline (PBS) solution shows an increased tensile strength of 12.1 MPa and strain at break of 2951%. The yield strength of this swollen TPU is 6.6 MPa, mimicking the mechanical property for uterosacral ligament tissue.

After 6 months in a shaker incubator at 37 °C, TPUs have degraded by 2.5 wt.% in a PBS solution with lipase enzyme.

SEM confirms the formation of aligned porous structure in the TPU scaffolds, mimicking the structure in ligament tissue. The porosity of the scaffolds is around 92%.

CONCLUSION

These new biodegradable TPUs show potential to be used in future uterosacral ligament tissue repair. The chemical structure of the TPUs may be modified in future work to increase their degradation rate.

DEVELOPMENT OF ANTI-LEISHMANIASIS DRUG AMPHOTERICIN B NANOCRYSTAL-BASED DISSOLVING MICRONEEDLE FOR INTRADERMAL DELIVERY

Jiawen Wang, Yaocun Li, Ryan F. Donnelly, Alejandro J. Paredes
School of Pharmacy, Queen's University Belfast, BT9 7BL, United Kingdom
email: a.paredes@qub.ac.uk (corresponding author's email)

INTRODUCTION

Leishmaniasis is a neglected parasite disease that endangers people living in tropical areas. Over 350 million people all over the world are exposed to the risk of being infected[1]. Amphotericin B (AmB) is the first-line drug for leishmaniasis treatment. Nanocrystals (NCs) are a nano-scale colloidal dispersion system consisting of only therapeutic agents and stabilisers. The highly drug loaded NCs have the potential for improving the dissolution performance of poorly soluble actives, as opposite to marketed liposomal formulations that have only a limited drug loading capacity. Microneedles (MNs) can be painlessly self-applied by patients to deliver the drug intradermally, which may have better patient adherence in comparison to infusion. We introduce the incorporation of NCs into dissolving MNs with potential application to treat leishmaniasis.

MATERIALS AND METHODS

The media milling method was used to produce the AmB nanosuspension. The experimental set up consisted of a glass vial containing the AmB and stabiliser solution, two 25 x 8 mm sized magnetic stirring bars and zirconia beads. Then the vial was placed on a Basic Magnetic Stirrer at 1500 rpm for 48 h. Afterwards, the magnetic bars and zirconia beads were separated from the nanosuspension using a mesh 48 µm pore sized sieve.

The AmB-NCs were obtained by freeze-drying the liquid nanosuspensions. The two-layered dissolving MNs were prepared. The moulds for MNs manufacture composed of 16 x 16 pyramidal-cubical shaped needles with the height of 850 µm. The first layer of the MN formulation contained NCs, 40% w/w of PVA, 40% w/w of PVP and deionised water. The second layer was composed of 30% w/w PVP and 1.5% w/w glycerol.

The dissolution of the AmB-NCs was tested and compared with the dissolution kinetics of AmB. The in vitro release study was carried out by using MN tips with the release medium PBS and 1% w/v SDS in a 37 ± 0.5 °C, 40 rpm incubator. At predetermined time points, 200 µL of samples were withdrawn and replaced immediately with the release medium. The concentration of AmB was determined by HPLC-UV.

The full-thickness skin was pre-collected from still born piglets and was carefully shaved using a razor for the *ex vivo* in-skin deposition study. MNs were inserted into the skin using manual force for 30 s. The MNs were maintained in place by a 15 g aluminum weight placed on the back of the MN baseplate to ensure the MN remained in situ for 24 h. After setting up the Franz cell system, the skin samples were collected at respective sampling time points. Then AmB was extracted with DMSO using a Tissue Lyser and quantified by HPLC-UV.

RESULTS

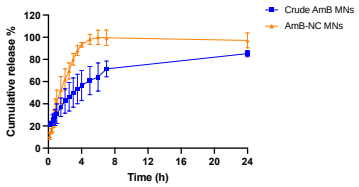

Figure 1 In vitro release profile of crude AmB MNs and AmB-NC MNs. (Means ± S.D., n = 3)

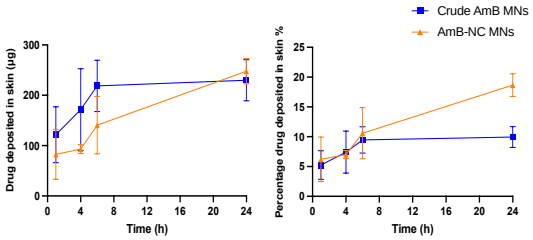

Figure 2 Ex vivo drug deposition in excised full-thickness neonatal porcine skin. (Means ± S.D., n = 3) 3 The percentage drug deposited in excised full-thickness neonatal porcine skin (AmB in skin/AmB in MNs, w/w). (Means ± S.D., n = 3)

DISCUSSION

The dissolution rate of AmB-NC MNs was faster than crude AmB MNs, with 100% cumulative release at 5 h. The AmB-NC MNs group from the drug in-skin deposition study achieved 247.86 ± 25.23 µg drug deposition and 18.66 ± 1.90% deliver efficiency at 24 h which is higher than the crude AmB MNs.

CONCLUSION

AmB-NC loaded dissolving MNs was fabricated by a bilayer casting technique. AmB-NC MNs showed faster dissolution rate and higher percentage drug delivery than crude AmB MNs.

REFERENCES

Organization WH. Control of leishmaniasis 2022 [WWW Document]. Key Facts. URL https://www.who.int/publications/i/item/wha60.13 (Accessed 14.6.2022).

DUAL FUNCTIONAL LBL ASSEMBLY NANOCOMPOSITE COATINGS FOR MECHANICAL REINFORCEMENT OF BONE TISSUE SCAFFOLDS AND ENHANCEMENT OF BONE DEFECR REPARATION VIA INCORPORATION OF THERAPEUTIC AGENTS.

McFerran, A.[1*], Lemoine, P.[1] Meenan, B.J.[1], Acheson, J.G.[1]
[1] Nanotechnology and Integrated Bioengineering Centre (NIBEC), School of Engineering, Ulster University Belfast
**e-mail: McFerran-A4@ulster.ac.uk*

INTRODUCTION

An estimated 2.2 million bone grafting surgeries are performed annually worldwide and with the incidence expected to rise by 13% each year[1], bone defect reparation is rapidly becoming one of the most common procedures in bone regenerative medicine. The limiting factors surrounding 'gold standard' autograft treatment highlights the need for a tissue engineered (TE) 'off-the-shelf" alternative. Through utilising layer-by-layer (LbL) assembly for the fabrication of thin films it is possible to add tremendous functionalisation. Single function coatings have been investigated previously[2] but combining them to create a novel coating with dual functionality has not yet been studied in detail. This work investigates the use of LbL functionalised coatings to improve the mechanical integrity of open cell structures coupled with the incorporation and release of reagents from the multilayers.

MATERIALS AND METHODS

1 wt.% of PDDA (poly (diallydimethylammonium chloride)), PAA (polyacrylic acid) and PEI (polyethylenimine), and 0.5 wt.% of powdered nanoclay (NC) were prepared in deionised water. Substrates were washed with 1 M NaOH and coated with a baseline coating consisting of $(PEI/PAA/PEI/NC)_n$ and a PDDA coating of PEI-$(PDDA/PAA/PDDA/NC)_n$. 7-day *in vitro* studies were performed to assess cytotoxicity. Methylene blue (MB) was used as a model drug at a concentration of 10 mg/L. Open cell structures were immersed in 10 mg/L MB solution for 24 hours (hrs) and desiccated for 24 hrs, followed by immersing in deionised water. The concentration of MB was determined at various time points by UV-Vis.

RESULTS

LbL coatings of PEI-(PDDA/PAA/PDDA/NC) match the compressive modulus of the baseline PEI coating, ~ 6 MPa at 60 QL. Interestingly, the porosity of the structures was not overly reduced to achieve an optimised modulus. Cell viability studies determined that the PDDA coating has a considerably higher cell viability with statistically significant differences (p < 0.0001) observed between the PEI and PDDA coatings. It was determined that MB was successfully incorporated and the 30 QL sample demonstrated a burst release of MB over the first 24 hrs and over 7 days reached a maximum release of ~ 80%. In contrast, ~ 60% of the MB was released from the 60 QL sample through the burst release phase and reached a maximum release of ~ 94% over 7 days.

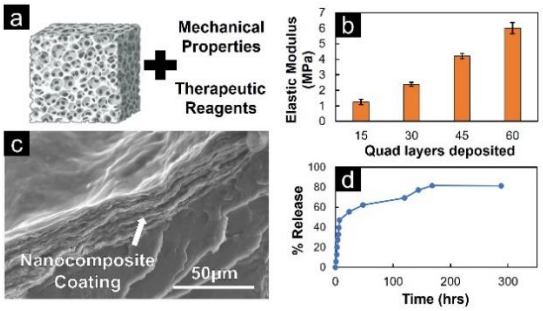

Figure 1 *a) Schematic diagram of project aim, b) elastic modulus of the PDDA coating as number of QL increase, c) SEM of 60 QL PDDA coating and d) release profile of MB from PDDA sample.*

DISCUSSION

LbL dual function PDDA coatings present a promising alternative to the PEI coating. The significant differences in cytotoxicity of the PEI and PDDA coatings may be explained by the differences in the structures, it has been reported previously that the quaternary amine groups present in PDDA are less cytotoxic compared to the primary amine groups in PEI[3]. For applications in bone tissue repair, it is desirable to provide a therapeutic system with a release profile consisting of a burst phase followed by a sustained release of the reagent, such as an antibiotic. The PDDA coatings demonstrated this release profile and therefore could potentially be utilised for the enhancement of bone tissue repair.

REFERENCES

1. Archunan, M. W. *et al. Cureus* **13**, e17705 (2021).
2. Acheson, J. G. *et al. Surf. Coat. Technol.* **458**, 129335 (2023).
3. Fakhrullin, R. F. *et al*. Cell Surface Engineering, Royal Society of Chemistry (2014).

A BRIGHT FUTURE: PHOTODYNAMIC ANTIMICROBIAL POLYMER FILMS WITH POTENTIAL USE AS ENDOTRACHEAL TUBE COATINGS FOR THE PREVENTION OF VENTILATOR ASSOCIATED PNEUMONIA

Irwin, R.N.[1], Wylie, M.P.[1], McCoy, C.P.[1]
[1] School of Pharmacy, Queen's University Belfast, 97 Lisburn Road, Belfast, United Kingdom.
email: (c.mccoy@qub.ac.uk)

INTRODUCTION

Within nosocomial environments, antibiotic resistance is prevalent, emanating mainly from biofilm formation following medical device insertion. A notable case is the introduction of an endotracheal tube as a means of mechanical ventilation, leading to the development of ventilator associated pneumonia. VAP has a higher mortality rate than other biofilm associated infections, attributed to its primary employment associated with intensive care patients (Diacona *et al*).

Antimicrobial biomaterial coatings represent a potential strategy for mitigation. Current coatings contribute to antibiotic resistance, governed by their inability to regulate release; a large initial burst subsequently followed by continuous elution at the subtherapeutic dose (Xiao *et al*). Therefore, 'smart' materials; capable of eliciting their antimicrobial effect upon response to exogenous or endogenous stimuli while modulating their action via on/off control are proposed. Photodynamic antimicrobial chemotherapy (PACT) employing light activated photosensitisers has shown promise. Upon irradiation, reactive oxygen species: singlet oxygen and oxygen based radicals are produced, adopting a catalytic multi-mechanistic action; photo-oxidizing biomolecules, contributing to cell lysis and disruption of cell physiology, inhibiting bacteria growth (Maldonado-Carmona *et al*).

In this work, photosensitiser loaded polymer films are fabricated, followed by microbiological characterisation with artificial sputum to assess their suitability as an endotracheal tube coating.

MATERIALS AND METHODS

Toluidine Blue O (TBO) and polycaprolactone were obtained from Sigma Aldrich. TBO was immobilised within the polymer *via* a solvent casting method. Artificial sputum was produced based on a method formerly defined by Sriramulu. A contact kill assay in conjunction with a repeat exposure test was performed: 100 µL of inoculated artificial sputum was placed on the surface of a 1 cm^2 film and irradiated for 4 hours under red light, followed by 24 hrs incubation at 37°C. Following incubation, day 1 samples were rinsed and sonicated to remove adherent bacteria and the resultant solution plated using the Miles & Misra method. Remaining samples were reinoculated, this procedure was repeated daily until day 7.

RESULTS

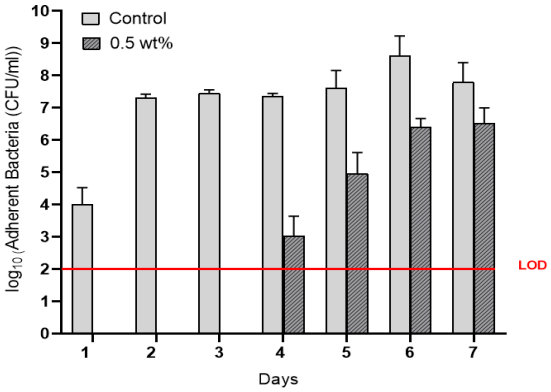

Figure 1. *Number of viable P. Aeruginosa (PAO1) adhered to the surface of 0.5 wt% TBO loaded polycaprolactone challenged daily for seven days with 100 µL of 1 x10^6 CFU/ml* inoculated *in artificial sputum. LOD indicates limit of detection as 100 CFU/ml*

DISCUSSION

Following insertion of the endotracheal tube, microbes can attach after a few hours with early onset VAP development within 48 hrs in the most critically ill (Park). The prognosis is often fatal due to the presence of antibiotic and multidrug resistant pathogens. This work has eliminated the need for antibiotics, with light mediated therapy resisting attachment of bacteria up to 4 days following insertion, providing patients with a much needed buffer period to overcome existing infections. Previous work has identified leaching of the photosensitiser as the antimicrobial mechanism of action with the profile indictive of burst release. Thus, future work will aim to slow the release, preserve the antimicrobial integrity of the films and extend the lifetime of the films beyond 4 days.

CONCLUSION

The TBO loaded polymer films successfully resisted adherence of *P.Aeruginosa* following 4 days of repeated inoculation.

REFERENCES

Diaconu *(et al.)*, Journal of Critical Care Medicine 4(2): 50–55, 2018.
Maldonado-Carmona (*et al.*), Photochemical & Photobiological Sciences 19(4): 445-461, 2020.
Park, Respiratory Care, 50(6): 742-765.
Sriramulu *(et al.)*, Journal of Medical Microbiology 54(7): 667-676, 2005.
Xiao *(et al.)*, Colloids and Surfaces B: Biointerfaces 192:110989, 2020.

Manufacturing and characterisation of a 3D printed polymer/ceramic scaffold for the repair and regeneration of critical-sized bone defects

Tiplady, S.[1], Lennon, A.[1] Larreneta, E.[2] Buchanan, F.[1] Manda, K.[1]
[1] School of Mechanical and Aerospace Engineering, Queen's University Belfast
[2] School of Pharmacy, Queen's University Belfast
email: stiplady01@qub.ac.uk

INTRODUCTION

As populations increase and age, increasing rates of osteoporosis and fragility fractures are decreasing the quality of life of patients whilst placing strain on healthcare systems worldwide[1]. Following most fractures, bone can heal spontaneously but in a number of cases (~1.9%), a therapeutic aid is required to achieve full healing[2]. Synthetic bone grafts are a promising approach to repair critically sized bone defects. An ideal scaffold would provide temporary mechanical stability, promote bone growth, and break down through natural pathways at the rate of new bone formation. A composite of poly (*l*-lactic-co-glycolic acid) (PLGA) and strontium doped tricalcium phosphate (Sr/TCP) may combine appropriate bioresorbability and osteoinductive potential to ensure such bioactivity and biocompatibility.

MATERIALS AND METHODS

Sr/TCP powders were fabricated using an aqueous precipitation method[3]. Synthesised powders were ground using a Retsch High Energy Ball mill and characterised using digital light scattering (DLS), Fourier-transform infrared spectroscopy (FTIR), X-ray diffraction (XRD) and scanning electron microscopy (SEM).

4x4x3mm **composite scaffolds** were fabricated using a GeSim Bioscaffolder. Initially TCP and Sr/TCP powders were dried in an oven and hand ground with a pestle and mortar to remove any agglomerates. PLGA pellets and dried ceramic powder were then cryogenically milled to form a composite powder in a freezer mill (Rondol Technology Ltd, UK) containing LN2. Scaffolds have been examined for morphology, filler dispersion, thermal and mechanical properties using SEM, µ-computed tomography (µ-CT), thermogravimetric analysis (TGA), and compression testing.

RESULTS

Micro **TCP and Sr/TCP powders** were analysed through ATR-FTIR, SEM and XRD analysis (Figure 1). Distinct peaks consistent with literature were observed (search/match software of the XRD data shows a high match for Sr/TCP consistent with literature as well as the ATR-FTIR data possessing characteristic peaks at approximately 947, 974 and 1120). Characteristic morphology of powders was, also, confirmed by SEM. DLS showed over 90% of particles were below 3 µm (D_{90}= 2.58 µm) and all particles were below 5 µm.

Composite bone scaffolds with reasonably consistent architecture were confirmed by SEM and optical microscopy (Figure 1), which showed pore sizes and strand widths between 530-620 µm and 340-430 µm respectively. TGA analysis of three samples at the beginning, middle, and end of print gave a filler of 8, 11, and 14.5%. Apparent compressive modulus of the composite scaffolds was 204 MPa in comparison to 181.5 MPa for a PLGA scaffold.

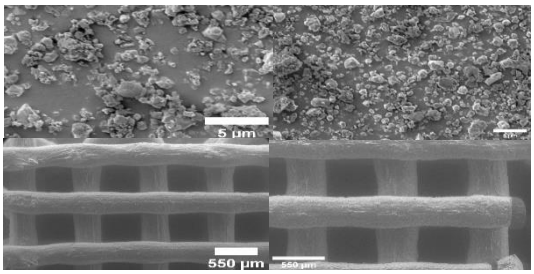

Figure 1 SEM imaging of TCP and Sr/TCP powders (top) and scaffolds produced (bottom).

DISCUSSION

This study demonstrated that doped-ceramic powders can be produced using an aqueous precipitation method in a relatively simple and effective manner. Controlling the wt% of doped material (in this case Sr) can be done by directly replacing Ca ions with Sr. To achieve consistent micro-sized particles, high energy ball milling is an effective method. DLS showed all particles were below a target size of 5 µm.

Production of composite bone scaffolds using a syringe-based printer has challenges. Notably the small nozzle size and the effect of a vertical chamber when using ceramic filler within a polymer matrix can cause blockages and uneven filler dispersion. TGA analysis has shown a reduction in filler percentage from the target of 20% to an average of 11% across a scaffold. However, consistent specimen-specific architecture can be obtained and an increase in mechanical properties using a polymer ceramic scaffold with this method is achievable.

REFERENCES

1. Chocholata et al, Materials, 12, p568, 2019
2. Mills et al, Acta Orthopeadica, 88, p434-439, 2017
3. Le Gars Santoni, B., et al., J. of the European Ceramic Society, 41(2), 2021.

Development of antibacterial urinary catheter for pH responsive hydrogel coatings released rifampicin

Jingyi Xu[1], **Colin P. McCoy, Matthew P. Wylie**

Email: [1]*jxu16@qub.ac.uk*

Background

Many patients who undergo long-term urinary catheterization become infected with bacteria which can lead to complications such as catheter-associated urinary tract infections (CAUTI). Catheters become blocked and encrusted due to bacterial species that produce urease. Urease can hydrolyze urea in urine to generate, raising the urinary pH and causing calcium phosphate and magnesium phosphate to deposit on the catheter surface [1]. Hydrogels have been further developed over the last 2-3 decades to become 'smart' or responsive hydrogels in which polymers or crosslinkers with special chemical properties can allow the hydrogel to become responsive to specific environmental triggers such as light, temperature, pH, ionicity, and enzymes [2]. In CAUTI, the alkaline shift in urinary pH can be exploited through development of catheter antibiotic-loaded hydrogel coatings which swell in response to alkaline pH, releasing antibiotics to eradicate adjacent bacterial cells. Therefore, pH responsive hydrogels as 'smart' materials have high potential research value in the treatment of CAUTI.

Methods

2-hydroxyethyl methacrylate (HEMA), ethylene glycol dimethacrylate (EGDMA), 2,2'-azo-iso-butyronitrile (AIBN) and methacrylic acid (MAA) were used to form hydrogels. Release of rifampicin from pH-responsive hydrogels was determined at neutral (pH 7) and alkaline (pH 10) conditions to simulate healthy and infected urine, respectively. Bacterial adherence assay was performed for unloaded and loaded rifampicin in the pH responsive hydrogels against *Escherichia coli* (*E. coli*) ATCC NSM59 and *Proteus mirabilis* (*P. mirabilis)* ATCC 51286 to determine the bacteria viability.

Results

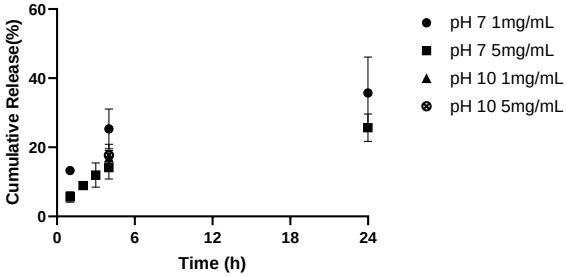

Figure 1*. Cumulative release curves of 1 mg/mL and 5 mg/mL rifampicin from p(HEMA) at pH 7 and 10. Each time point represents an average ± SEM (n = 5).*

MAA possesses an ionizable carboxylic acid group which becomes anionic in alkaline pH leading to electrostatic repulsion between neighboring MAA polymeric chains. This resulted in increased swelling of MAA-incorporated polymers in alkaline buffer compared to p(HEMA). The increased swelling of MAA-incorporated gels in alkaline pH resulted in a more rapid release of rifampicin compared to neutral pH media with >90% drug release within 6 h compared to ~50% at pH 7 for 10% MAA gels. However, during initial bacterial studies the more rapid release of rifampicin from MAA-incorporated gels did not lead to a significant improvement in reducing bacterial adherence compared to non-stimuli responsive HEMA gels.

MULTIFUNCTIONAL NANOCOMPOSITES FOR BONE IMPLANT APPLICATIONS

Dan Sun[1], Miaomiao He[2], Li Zhang[2]

[1] Advanced Composite Research Group (ACRG), School of Mechanical & Aerospace Engineering, Queen's University Belfast, UK BT9 5AH

[2] Analytical & Testing Center, Department of Orthopedic Surgery and Orthopedic Research Institute, West China Hospital, Sichuan University, Chengdu 610065, China

email: d.sun@qub.ac.uk

The use of PEEK has grown exponentially in the biomedical field in the past few decades and has rapidly transformed a large section of the medical devices landscape. However, the bioinertness of PEEK remains a limitation for its bone repair applications [1]. The increasing demand for enhanced treatment efficacy calls for innovation in bone implants that can offer fast bone integration as well as other desirable therapeutic functions. As such, modification of PEEK implants has progressively shifted from offering desirable mechanical properties, enhancing bioactivity/fast osteointegration, to more recently, tackling post-surgery bacterial infection/biofilm formation, modulation of inflammation and management of bone cancers [2]. Such progress is also accompanied by the evolution of the PEEK manufacturing technologies, to meet the ever-increasing demand for more patient specific devices.

In this paper, the authors will provide an overview of the PEEK based bone inplants. We will start with introducing the modification of PEEK using graphene and/or its derivatives graphene oxide, and reveal how such modification can improve the bioactivity and mechanical properties of the resulting composite implants. We will then demonstrate 3D printing of PEEK/graphene nanocomposites scaffold and how photothermal conversion properties of the graphene based filler materials can be deployed for multimodal bone therapeutics such as bone cancer management, anti-bacteria and drug delivery applications.

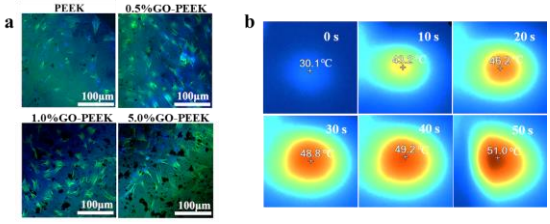

Figure 1 (a) CLSM images of BMSCs demonstrating bioactivity of the PEEK and GO-PEEK implants in vitro and (b) photothermal effect of 0.5%GO-PEEK upon laser irradiation (0.31 W/cm2 for 10 min)

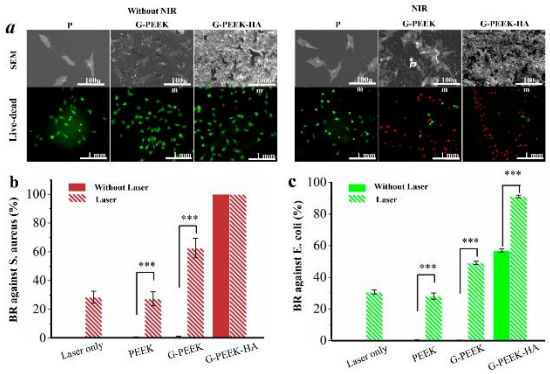

Figure 2 The growth of MG-63 (a) and antibacterial property (b) of 3D printed PEEK, G-PEEK and G-PEEK-HA scaffolds with and without NIR irradiation

REFERENCES

1. He *et al.*, Acta Biomaterilia: 129, 18-32, 2021

2. He et al., *Composites Part B: Engineering* 246, 110266, 2022

COMPUTATIONAL EVALUATION OF SKULL AND SPRING PARAMETERS IN SPRING ASSISTED SAGITTAL SYNOSTOSIS CORRECTION

Jacob, Jenson, Bozkurt, Selim
School of Engineering, Ulster University, Belfast, United Kingdom
email: jacob-j1@ulster.ac.uk

INTRODUCTION

Craniosynostosis is a rare condition which happens when one or more cranial sutures fuse prematurely during infancy[1]. The most prevalent kind of craniosynostosis is sagittal craniosynostosis[2]. Closure of the sagittal suture prematurely leads to installed lateral development and unhindered anteroposterior growth given the presence of other open sutures causing a narrow and elongated cranium known as scaphocephaly[2].
Lauritzen et al developed a novel treatment method for scaphocephaly in 1998[3] by incorporating springs that allowed the cranium to expand and remould. Metal springs were inserted along the osteotomy boundaries where the incisions were made which is both functionally and cosmetically beneficial. However, owing to insufficient knowledge about how various parameters affect the post-op outcome to what degree, the final shape outcomes remain relatively unpredictable. The purpose of this work was to develop FEA models of spring-assisted cranioplasty with various parameters and study their effects on the post-operative results.

MATERIALS AND METHODS

The properties of the skull and surgical parameters were obtained from the available literature. The skull is modelled using skull properties acquired. A sensitivity analysis of the mesh is performed to determine the element size for discretization. The surgical parameters were added to the model, and then the analysis was conducted. The results for the immediate post-op cephalic index were recorded, and sensitivity analysis is performed.

RESULTS

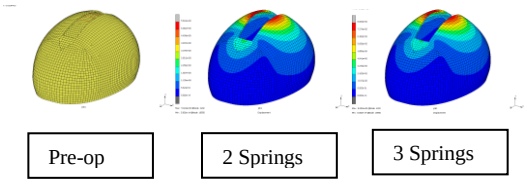

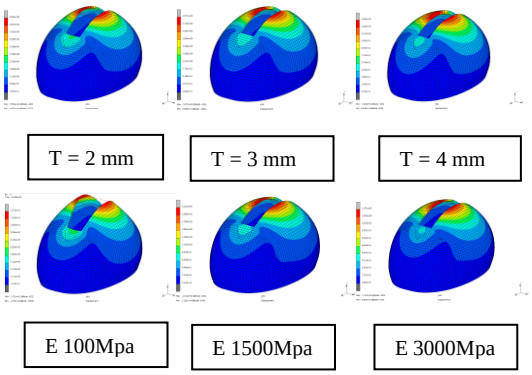

Figure 1. Post-surgical displacement for different thicknesses, elastic moduli, and the number of springs.

DISCUSSION

The number of springs had the greatest impact on immediate post-operative outcomes according to the analysis. Three springs are more efficient than just two. Material properties of the skull were another significant contributor to the outcomes. The improvement in the cephalic index is greatest for those with the lowest Young's modulus. This shows that the younger the patient, the better the outcome, as Young's modulus increase with age.

CONCLUSION

The insights gained from this analysis could be used to plan surgery according to the patient's age and skull characteristics. The effect of various parameters on the surgical outcome can be studied to fine-tune surgical procedures.

REFERENCES

[1] D. Johnson and A. Wilkie, "Craniosynostosis", European Journal of Human Genetics, vol. 19, no. 4, pp. 369-376, 2011.
[2]A. Sharma, K. Fagan and J. Kucera, "Pictorial Review of Craniosynostosis", Journal of Radiology Nursing, vol. 41, no. 1, pp. 38-43, 2022.
[3]C. Lauritzen, Y. Sugawara, O. Kocabalkan and R. Olsson, "SPRING MEDIATED DYNAMIC CRANIOFACIAL RESHAPING: Case report", Scandinavian Journal of Plastic and Reconstructive Surgery and Hand Surgery, vol. 32, no. 3, pp. 331-338

BIOMATERIAL COATINGS WITH LUBRICIOUS, SLIPPERY PROPERTIES FOR IMPROVED URINARY CATHETER PERFORMANCE

Ross, J.[1], McCoy, C.[2] , Wylie, M.[3]
[1] School of Pharmacy, Queen's University Belfast, Belfast BT9 7BL, UK
[2] Queen's University Belfast, Belfast BT9 7BL, UK
3 Queen's University Belfast, Belfast BT9 7BL, UK
email: jross20@qub.ac.uk

INTRODUCTION

Intermittent catheterisation is used to facilitate urine drainage. Although designed as single use, reuse of intermittent catheters (ICs) is a common practice to reduce environmental impact and healthcare costs[1]. The repeated insertion and removal of ICs increases the risk of urethral trauma, with non-sterile reuse also increasing patient susceptibility to catheter-associated urinary tract infections (CAUTIs)[2]. This project aims to develop a surfactant-incorporated urinary catheter coating to impart the unique tribological and antimicrobial properties of cationic surfactants to the resulting coating[3]. A range of polymerizable phosphonium-based surfactants with varying hydrocarbon pendant and spacer groups have been synthesized. The optimal pendant and spacer group size was investigated to enhance both lubricious and wettability properties of the resulting hybrid coatings when incorporated with 2-hydroxyethyl methacrylate (HEMA).

MATERIALS AND METHODS

Phosphonium-based surfactant monomers were synthesized via nucleophilic substitution of bromoalkenes with trialkylphosphines. Ionic liquids were synthesized and characterised using nuclear magnetic resonance (NMR) and Fourier-transform infrared (FTIR) spectroscopy. Thermal polymerization was used to synthesise copolymer films of HEMA and surfactant monomer, using ethylene glycol dimethacrylate (EGDMA) crosslinker and azobisisobutyronitrile (AIBN) initiator (Table 1). ATR-FTIR confirmed successful polymerization. Copolymer swelling studies were performed at 37 ℃, pH 7.4 to mimic the physiological conditions. Contact angle measurements were determined via the captive bubble method. Adherence assays investigated the anti-adherent properties of the copolymer gels against *Staphylococcus aureus* ATCC 29213.

RESULTS

Swelling studies have shown that increasing copolymer composition of surfactant monomer results in a decrease in swelling ability of the gel, with 34.6% (H1) compared to 29.4% (H3). Contact angle measurements have shown that increasing copolymer composition of surfactant monomer results in a decrease in contact angle, with 33.9° (H1) compared to 31.6° (H2) and 33.2° (H3).

Preliminary adherence observations have shown a reduction in viable *S. aureus* by 36.9-60.5% on surfactant-incorporated films compared to p(HEMA).

Table 1: *Feed composition to prepare 10 g films.*

Hydrogel symbol	Component weight / g			
	HEMA	$P_{888allyl}Br$	EGDMA	AIBN
H1	9.95	0.00	0.10	0.10
H2	8.80	1.00	0.10	0.10
H3	7.80	2.00	0.10	0.10

DISCUSSION

As surfactant monomers are relatively more hydrophobic than HEMA, increasing copolymer compositions of surfactant monomer was expected to reduce copolymer swelling[4]. A higher contact angle for H2 than H1 was expected due to increasing hydrophobicity, but this was not observed. It is possible that surfactant monomer composition is not substantial enough to change copolymer surface properties. An increase in contact angle was observed from H2 to H3. Further adherence studies using *E. coli* and *S. aureus* are expected to display the broad spectrum antimicrobial and anti-adherent properties of these copolymers.

CONCLUSION

HEMA hydrogels incorporated with surfactant-based monomers have different properties to 100% HEMA hydrogels. Developing a urinary catheter coating including surfactant-based functionality may increase catheter lubricity and bacterial anti-adherent properties leading to improved patient quality of life and reduced risk of CAUTI development.

REFERENCES

1 Wilks *et al*., *Neurourol. Urodynam*. 39: 907-915, 2020.
2 Prieto-Fingerhut *et al*., *Rehabil. Nurs*. 22: 299-302, 1997.
3 Anvari *et al*., *J. Mol. Liq.* 221: 685-690, 2016.
4 Hermitte et al., *J. Colloid Interface Sci*. 272: 82-89, 2004.

PEKK-HYDROXYAPATITE COMPOSITES FOR PATIENT MATCHED 3D PRINTED MEDICAL IMPLANTS

Hasson, F.*[1], Boyd, A. [1], Krzysztof, R. [1], Mcllagger, A. [1]
[1] Ulster Univeristy
hasson-f3@ulster.ac.uk

INTRODUCTION

Polyetherketoneketone (PEKK) is a novel biomaterial that is of particular interest for replacing metallic implants due to its excellent biocompatibility and mechanical properties. It is a high-performance thermoplastic polymer[1] which offers mechanical properties that are more closely matched to bone than other prosthetic materials, providing a similar modulus of elasticity to help prevent stress shielding and fatigue fractures due to cyclic loading[2], improving overall patient outcomes. However, PEKK is non-biodegradable and bioinert, leading to fibrous encapsulation of the implant and weak osteointegration at the bone-implant interface[345]. The three main strategies to improve the osteointegration of PEKK are the addition of bioactive fillers, surface modification, and the utilisation of porous structures[4]. The aim of this study is to produce a polymer-ceramic composite material, utilising the addition of bioactive hydroxyapatite (HA) as a filler. HA is chemically similar to the mineral component of bone and is therefore osteoconductive and promotes osteointegration with the implant [6].

MATERIALS AND METHODS

The samples for the study were produced using fused filament fabrication (FFF) 3D printing on a modified Ultimaker 2+. Hydroxyapatite filler was added to the PEKK polymer matrix at various weight percentages (0wt%, 10wt%, 20wt%, and 30wt%). A range of analytical characterisation methods were employed in this preliminary study including scanning electron microscopy with energy dispersive x-ray analysis (SEM-EDX), micro computed x-ray tomography (µCT), Fourier transform infrared spectroscopy (FTIR), and thermal gravimetric analysis (TGA).

RESULTS AND DISCUSSION

SEM-EDX analysis revealed HA particles distributed across the surface of the 3DP samples. Furthermore, EDX analysis confirmed the homogeneous presence of calcium (Ca) and phosphate (P) elements. The HA particle size was shown to be in the range 25-180µm. µCT analysis confirmed that the HA particles were also distributed through the bulk of the polymer matrix. FTIR analysis revealed the presence of PO_4^{3-} peaks between 900-1150 cm^{-1}, which helps to confirm the presence of HA on the surface. All the peaks indicative of PEKK were also observed in the FTIR spectra. TGA confirmed the expected wt% of filler in each 3DP sample.

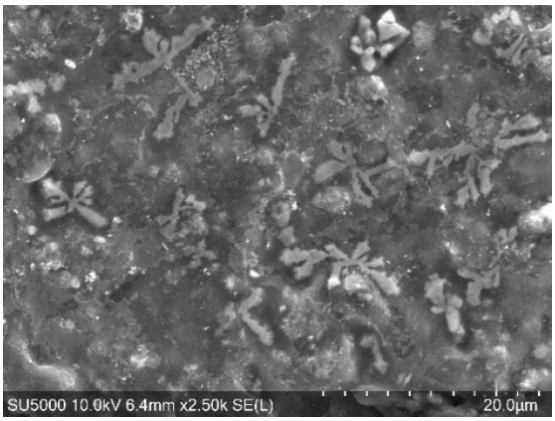

Figure 1 SEM image of PEKK sample containing 20wt% HA at a magnification of x2.5k.

CONCLUSION

This study confirmed the presence of bioactive HA in the bulk and on the surface of PEKK-HA composite 3D printed samples. This suggests that PEKK-HA composite materials have the potential to be useful for medical implants. Further investigation is required, particularly regarding the effect of the filler on mechanical properties and on the *in vitro* properties of the composites. Additionally, it may be beneficial to dope the HA with bioactive ions such as magnesium (Mg) and silicon (Si) to further improve the bioactivity of the implant, which will also be a major consideration of this project going forward.

REFERENCES

1. Alqurashi, H. *et al.* Polyetherketoneketone (PEKK): An emerging biomaterial for oral implants and dental prostheses. *J Adv Res* **28**, 87–95 (2021).
2. Moore, W. R., Graves, S. E. & Bain, G. I. Synthetic bone graft substitutes. *ANZ J Surg* **71**, 354–361 (2001).
3. Ji, Y., Yu, X. & Zhu, H. Fabrication of mg coating on peek and antibacterial evaluation for bone application. *Coatings* **11**, (2021).
4. Yuan, B. *et al.* Comparison of osteointegration property between PEKK and PEEK: Effects of surface structure and chemistry. *Biomaterials* **170**, 116–126 (2018).
5. Zheng, J. *et al.* Additively-manufactured PEEK/HA porous scaffolds with highly-controllable mechanical properties and excellent biocompatibility. *Materials Science and Engineering C* **128**, (2021).
6. Li, S. *et al.* Porous polyetheretherketone-hydroxyapatite composite: A candidate material for orthopedic implant. *Composites Communications* **28**, 100908 (2021).

ENHANCED ANTI-BIOFILM AND ANTI-PROTEIN ADSORPTION PROPERTIES OF LIQUID-INFUSED SILVER-POLYTETRAFLUOROETHYLENE COATINGS

Ruolan, Chen.[1], Xiao,Teng. [2], Coin P. McCoy.[3], Shuai, Zhang.[4]
[1] School of Pharmacy, Queen's University Belfast, BT9 7BL Belfast, UK
email: shuai.zhang@qub.ac.uk

INTRODUCTION

Medical device-associated infections (MDIs) remain a major concern globally. As a basic survival strategy, microorganisms tend to colonise and grow on surfaces, in the form of biofilms. Current strategies to prevent MDIs mainly include antimicrobial, anti-adhesive, and combinatorial approaches. However, their long-term use in biomedical applications and the emergence of silver/antibiotic-resistant pathogenic bacteria remain to be addressed. On exposure to a complex physiological environment, proteins may rapidly adsorb onto device surfaces and redefine the surface properties, acting as a conditioning film and affecting bacterial adhesion.

METHODS

A slippery liquid-infused silver-polytetrafluoroethylene (AgFP) coating was fabricated via a spontaneous polycondensation of 1H,1H,2H,2H-perfluorooctyltriethoxysilane (PFOTES) onto an electroless AgF sublayer. The anti-biofouling properties were investigated by adsorption of Escherichia coli, Staphylococcus aureus, fibrinogen, and bovine serum albumin.

RESULTS

As evident after 24 h of co-culture with E. coli or S. aureus, the Ag and AgF surfaces still demonstrated extensive bacterial adhesion (Fig. 1). The incorporation of PTFE particles altered the anti-adhesion efficacy after and minimum bacterial adhesion was observed when the PTFE concentration reached 10 mL/L (AgF-2), reducing 60.6% and 30.3% of E. coli adhesion, 51.9% and 22.1% of S. aureus adhesion, respectively, when compared with SS and Ag coating. Notably, a further ~70% reduction in CFU was observed on the AgFP coating regardless of its weakest anti-bacterial activity. The results suggest that the liquid-like AgFP surface could effectively reduce bacterial accumulation and inhibit biofilm formation.

To mimic the complexities of the biological environment, the antibiofilm performance of the coatings was challenged with a protein-bacteria co-deposition model. The AgF-2 coating with verified best anti-adhesion performance (Fig. 1) was used as a reference. After introducing proteins into the media, all the surfaces experienced a dramatic increase in biofilm coverage (Fig. 2).

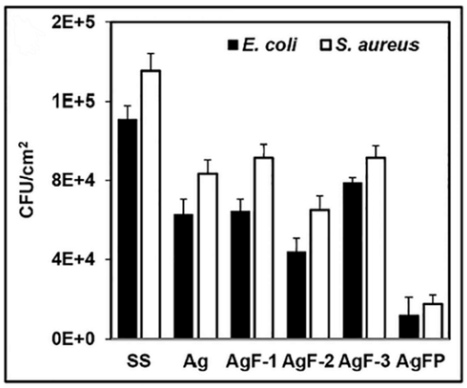

Figure 1 Quantitative counts of viable bacterial cells adhering to different surfaces after 24 h of incubation.

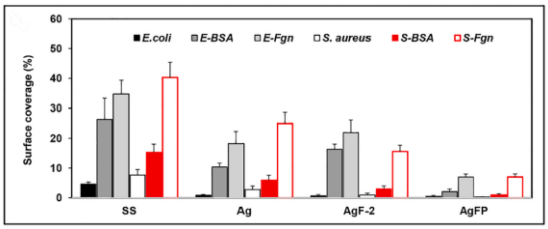

Figure 2 comparison of surface coverage of biofilm on different coatings after 24 h (n = 6, bars represent standard deviation of the mean).

CONCLUSION

In summary, compared with traditional Ag and AgF coatings, the AgFP coating showed ultralow adhesion for both bacteria and proteins. Protein-bacteria co-deposition experiments showed that the AgFP coating was able to significantly inhibit biofilm formation in near-real conditions.

REFERENCES

Dunne, W. M., Bacterial adhesion: seen any good biofilms lately? Clin. Microbiol. Rev. 15 (2): 155–166, 2002.

P. Singha (et al.), A review of the recent advances in antimicrobial coatings for urinary catheters, Acta Biomater. 50: 20–40, 2017.

J. Palmer (et al.), Bacterial cell attachment, the beginning of a biofilm, J. Ind. Microbiol. Biotechnol. 34 (9): 577–588, 2007.

MODELLING THE PROPERTIES OF 3D PRINTED PARTS MADE WITH ADVANCED MATERIALS

O'Donnell, E.*[1], Krzysztof, R. [1,] Boyd, A. [1]
[1] School of Engineering, Ulster University, York Street, Belfast, BT15 1ED (UK).
**odonnell-e19@ulster.ac.uk*

INTRODUCTION

Polyaryletherketones (PAEKs) are a group of high-performing semicrystalline thermoplastic polymers used in Additive Manufacturing (AM) that possess the unique ability to be manufactured as amorphous or partially crystallized bodies [1]. Crystallization time serves as a critical parameter for printing PAEK materials. In Fused Filament Fabrication (FFF), material deposition should ideally occur upon a previously deposited amorphous material to create strong interaction between layers. If deposition occurs upon a fully crystallized layer, bonding is weak- a major concern for PEEK as the homopolymer crystallizes rapidly. Controlling crystallization kinetics serves as a promising tool for the development of enhanced materials differentiated by their enhanced properties compared to the materials they may replace, such as human cortical bone [2]. For semi-crystalline polymers, crystallization is controlled by the nucleation process when temperatures approach the melting point and by segmental diffusion at lowered temperatures. Selection of materials with moderate crystallization kinetics is a better method for controlling crystallization as it allows for adjustment of the mechanical properties according to the needs of specific applications [3]. This work here aims to study a range of new Ppolyetheretherketone/Polyethylenimine (PEEK/PEI) polymer blends and identify suitable candidates that can be processed and mixed as composites to deliver suitable products through 3D printing for a range of application areas including medical devices.

MATERIALS AND METHODS

A classification model will be developed for neat materials and composites which will allow us to link material properties of the 3DP parts with crystallisation kinetics. PEEK/PEI material blends will be developed and evaluated based on peak crystallization and the 3DP process around crystallisation temperature peak- dividing them into 3 groups- slow, moderate and fast crystallization kinetics. Suitability of the model will be validated by comparison with semi-crystalline materials currently available on the market. Test samples will be printed on an OP^{TM}HT printer under various chamber conditions with the unique ability to control the temperature of a single layer and the mechanical, thermal and chemical properties will be studied. Assessment on the influence of 5-20wt% of two types of filler (carbon fiber (CF) and hydroxyapatite (HA)) on the kinetics of crystallization will be carried out as precursors for implants and injection molds using a range of characterization methods including scanning electron microscopy with energy dispersive x-ray (SEM-EDX), micro computed x-ray tomography (µCT), Fourier transform infrared spectroscopy (FTIR), thermal gravimetric analysis (TGA), differential scanning calorimetry (DSC) and dynamic mechanical analysis (DMA). This will provide fine-tuning capabilities of properties and optimal conditions of make-to-measure medical implants with improved flexibility, bioactivity and impact resistance as well as injection moulds with improved thermal resistance and elastic modulus.

RESULTS AND DISCUSSION

A preliminary SEM-EDX study on PEKK-Hydroxyapatite (HA) exemplar samples with HA content 5-20wt% revealed increasing homogeneous content of calcium and phosphate throughout the samples and the filler content directly influenced the crystallization kinetics by acting as nucleation agent, accelerating the crystallization rate.

Figure 1. SEM image of PEKK-HA with 20%wt HA showing visible HA distribution and crystallisation.

CONCLUSION

Currently, mainstream materials for 3DP are chosen based on the properties achieved by injection molding with an expectation of performance replication. However, separate material classifications are necessary for accurate property prediction to achieve the complex needs of 3DP for a range of purposes with no warping, good interlayer connection and adhesion, especially in Z direction, thus optimising their mechanical performance and utilisation.

REFERENCES

[1] S. Najeeb, M. S. Zafar, Z. Khurshid, and F. Siddiqui, "Applications of polyetheretherketone (PEEK) in oral implantology and prosthodontics," *J Prosthodont Res*, vol. 60, no. 1, pp. 12–19, Jan. 2016, doi: 10.1016/J.JPOR.2015.10.001.

[2] T. Choupin, B. Fayolle, G. Régnier, C. Paris, J. Cinquin, and B. Brulé, "A more reliable DSC-based methodology to study crystallization kinetics: Application to poly(ether ketone ketone) (PEKK) copolymers," *Polymer (Guildf)*, vol. 155, pp. 109–115, Oct. 2018, doi: 10.1016/J.POLYMER.2018.08.060.

[3] K. Rodzeń, A. McIlhagger, B. Strachota, A. Strachota, B. J. Meehan, and A. Boyd, "Controlling crystallization: A key factor during 3D printing with the advanced semi-crystalline polymeric materials PEEK, PEKK 6002 and PEKK 7002," *Institute of Macromolecular Chemistry*, pp. 1–26, 2022, doi: Submitted and in review.

IMPLANTABLE DEVICES FOR CANCER TREATMENT

Magill,E. [1], **Larrañeta, E.** [1], **Donnelly, R.F.** [1]

[1] School of Pharmacy, Queen's University Belfast, 97 Lisburn Road, Belfast BT9 7BL
email: emagill07@qub.ac.uk

INTRODUCTION

Implantable chemotherapeutic devices have the ability to overcome current treatment problems such as limited bioavailability and systemic side effects[1]. The treatment aim will be glioblastoma, the most common and malignant brain cancer that is notoriously hard to treat[2]. The recurrence rate is around 90%[3]. Here we design an implant that can reach deep tissues, with drug release concentrated at the tip of the device for a localised effect. The use of biodegradable polymers overcomes surgical removal. Such devices are capable of reducing high social and medical burdens, increase patient quality of life, and have the potential to be refillable. Presented here are the preliminary investigations on implant design.

MATERIALS AND METHODS

For the implant bodies poly-caprolactone (50kDa) was mixed with dichloromethane (DCM) to achieve 30%w/v. The body is made by solvent casting the mixture around a rotating 1mm diameter metal rod. Fused deposition modelling (FDM) uses poly-lactic acid (PLA) to print the tip onto a porous membrane (3DP tips). Membranes are formed by mixing PLA with a variety of hydrophilic polymers. Polymer compositions are mixed with DCM to create 3%w/v solutions which are cast to make membranes. Implants filled with 1mg/mL fluorescein isothiocyanate-dextran 4kDa (FITC Dextran). *In vitro* release media is 10mL of PBS solution incubated at 37°C.

RESULTS

Initial release studies found that implants with 3DP tips showed an improved release profile compared to tips formed by solvent casting. Of the membranes investigated, three were chosen as the best to continue research with. This was based on ease of implant assembly, as well as release profiles. A new release study was carried out for 14 days with these membranes (*Figure 2).* All exhibited similar profiles.

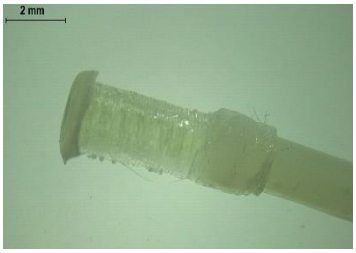

Figure 1. Microscope image of assembled implant emphasising the 3DP tip and membrane.

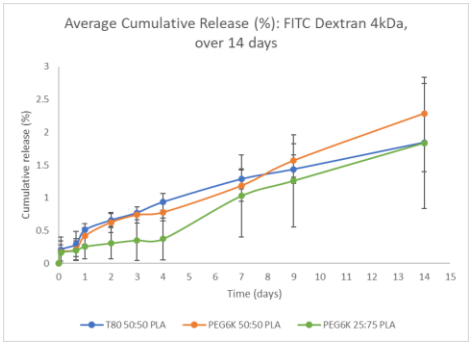

Figure 2. *In vitro* cumulative release profiles from implants with three different membranes over 14 days.

DISCUSSION

The improved release from the 3DP tips is due to the homogenous dispersion of pores on the membrane surface. Using hydrophilic polymers in the membranes enables these pores to enlarge in solution and encourages release from the implant. The larger deviation in particular membranes is possibly due to the formation of holes when submerged in solution. The studies were ceased due to the slow release, indicating modification needed. This has led to the current investigation of 3DP tips with larger membrane surface areas.

CONCLUSION

Porous membranes provide the ability to control release, with the possibility to tailor release to suit various treatments. These early results have provided a good basis to move forward and modify implants based on both kinetics and practicality in manufacture. The implant bodies provide an impermeable drug house so the treatment will continue as long as the materials last. The design is ideal for future progression to a refillable device.

REFERENCES

Chew et al, Advanced Healthcare Materials, 1600766, 6(2), 2017.
Nam et al, Journal of Oncology Practice, 13(10) 629-638, 2017.
Chen et al, Frontiers in Oncology, 641-878, 2021.

3D PRINTING OF PEEK APATITE COMPOSITES FOR ORTHOPEADIC IMPLANTS

McMullan, R[1], Golbang, A[1] and Boyd, A R[1],
[1] School of Engineering, Ulster University, York Street, Belfast. BT15 1ED (UK).
**e-mail: Monachan-R@ulster.ac.uk*

INTRODUCTION

Neck and lower back pain is a common issue caused by several factors such as injuries, accidents, etc., but spinal disorders such as degenerative scoliosis or degenerative disc disease are responsible for many hospital referrals and affects over 80% of the population worldwide [1]. To combat these conditions spinal fusion surgery can be undertaken [2]. According to Grand view research, the spinal implants and devices market has been valued at $12.4 billion in 2021 and is projected to grow at a rate of 5.1% from the period 2022 to 2030 [3]. Metallic implants are commonly used to make the fixation devices for spinal fusion surgeries due to their excellent mechanical properties but complication such as stress shielding was observed [4]. The use of titanium is limited due to artefacts created during imaging and can create artefacts in the results of computerised tomography (CT) and magnetic resonance imaging (MRI) [4]. Polymeric materials, such as Polyetheretherketone (PEEK) offer new opportunities to combat these issues as an suitable alternative to metal based materials [5]. PEEK is biocompatible, has high mechanical strength, high temperature resistance, fatigue resistance, and can be sterilised making it a perfect candidate for healthcare applications, especially orthopaedics. PEEK is considered as bioinert, but Rodzen *et al.* demonstrated that by adding bioactive agents such as hydroxyapatite (HA) into the PEEK matrix solves this problem and can help with aiding direct bone apposition [5]. The aim of this project is to develop a bioactive 3D printed composite material from PEEK HA apatite that will find application for spinal fusion and other orthopaedic applications. The application of 3D printing here opens up the possibly of patient specific implants and devices.

MATERIALS AND METHODS

A modified commercial printer Ultramaker 2+ was used to print the 3D samples of PEEK with weight percentage loadings of HA (0%, 10%, 20% and up to 30%). The samples were them characterised using Fourier transform infra-red spectroscopy (FTIR), Thermal gravimetric analysis (TGA), Scanning Electron Microscope (SEM), Energy Dispersive X-ray (EDX) analysis and MicroCT to determine the chemical composition, thermal properties, crystallographic structure and physical nature of the PEEK HA composite material.

RESULTS

TGA results confirm the expected composition (0-30% HA by weight) was maintained during extrusion and with the 3D printed samples. MicroCT results highlighted the distribution and content of HA in the sample, with particles of between 30-200 microns in diameter distributed evenly throughout the samples. No HA was detected in the 0% HA sample (pure PEEK). FTIR spectra and SEM images showed evidence of HA on the surface, with phosphate peaks (PO_4^{3-}) present between 1200-900 cm^{-1} and 650-500 cm^{-1} in the FTIR spectra for the 10, 20 and 30% HA loaded PEEK samples. SEM-EDX analysis confirmed the HA material is evenly distributed throughout and on the surface of the sample as evidenced by the calcium and phosphorus elemental maps.

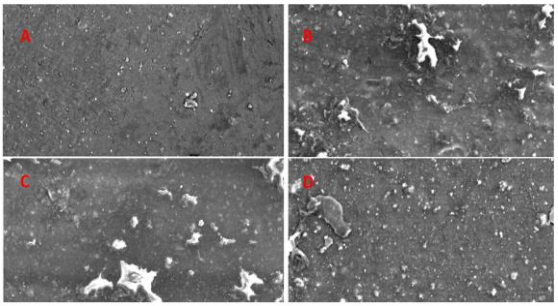

Figure 1 SEM images of PEEK HA – A) 0%, B) 10%, C) 20%, D 30% in 1K magnification.

DISCUSSION

From the preliminary experiments, results indicate that 3D printing of PEEK/HA composites up to 30% HA can be achieved as confirmed by characterisation methods using thermal, physical and chemical analytical methods.

CONCLUSION

These preliminary results indicate that these 3D printed materials have the potential be used in orthopaedic applications, such as spinal fusion devices. Further studies needs to be conducted to understand further their mechanical, chemical and physical nature along with targeted *in vitro* characterisation.

REFERENCES

1. D. I. Rubin, "Epidemiology and risk factors for spine pain," *Neurol Clin*, vol. 25, no. 2, pp. 353–371, May 2007, doi: 10.1016/J.NCL.2007.01.004.
2. E. Provaggi, C. Capelli, J. J. H. Leong, and D. M. Kalaskar, "A UK-based pilot study of current surgical practice and implant preferences in lumbar fusion surgery," 2018, doi: 10.1097/MD.0000000000011169.
3. "Spinal Implants & Devices Market Size, Share & Trends Analysis Report By Product, By Technology, By Surgery Type, By Procedure Type, And Segment Forecasts, 2022 - 2030," *Report ID: GVR-1-68038-031-6*.
4. B. I. Oladapo, S. O. Ismail, B. Oluwole, F. T. Omigbodun, M. A. Olawumi, and M. A. Muhammad, "Lattice design and 3D-printing of PEEK with Ca10(OH)(PO4)3 and in-vitro bio-composite for bone implant".
5. K. Rodzeń *et al.*, "The Surface Characterisation of Fused Filament Fabricated (FFF) 3D Printed PEEK/Hydroxyapatite Composites," *Polymers (Basel)*, vol. 13, no. 18, p. 3117, Sep. 2021, doi: 10.3390/POLYM13183117.

Development of 3D-printed subcutaneous implants using concentrated polymer/drug solutions

Picco, C.J.[1], Utomo, E.[1], McClean, A.[1], Dominguez-Robles, J.[1], Anjani, Q.[1], Volpe-Zanutto, F.[1], McKenna, P.E.[1], Acheson, J.G.[2], Dessislava, M.[3], Donnelly, R.F.[1], Larrañeta, E.[1]*

[1]School of Pharmacy, Queen's University Belfast, 97 Lisburn Road, Belfast BT9 7BL, United Kingdom

[2] Nanotechnology and Integrated Bioengineering Centre (NIBEC), School of Engineering, Ulster University, United Kingdom

[3] Wellcome-Wolfson Institute for Experimental Medicine, Queen's University Belfast, Belfast, United Kingdom

email: cpicco01@qub.ac.uk

INTRODUCTION

Implantable drug-eluting devices that provide therapeutic cover over an extended period of time following a single administration have potential to improve the treatment of chronic conditions. These devices eliminate the requirement for regular and frequent drug administration, thus reducing the pill burden experienced by patients (Quarterman, 2021). Furthermore, the use of modern technologies, such as 3D printing, during implant development and manufacture renders this approach well-suited to produce highly tuneable devices that can deliver treatment regimens which are personalised for the individual (Khaled, 2014). The objective of this work was to formulate subcutaneous implants loaded with a model hydrophobic compound, olanzapine (OLZ) using robocasting 3D-printing technique.

MATERIALS AND METHODS

OLZ, poly(caprolactone) (PCL) and poly(ethylene)glycol (PEG) were dissolved in dichloromethane and mixed at 3000 rpm for 3 min using a SpeedMixer™ DAC 150.1 FVZ-K. The formulations were loaded into a 10 mL plastic syringe with a 20-gauge tip which was then attached to the 3D printer head. Each implant was designed using computer-aided design (CAD) software, Tinkercad® and printed using an Allevi® 2 Bio-printer. Print speed was maintained at 2 mm/s, layer height was 0.6 mm and nozzle pressure were 38 psi.

RESULTS

Rod-shaped implants with dimensions measuring 1.5 mm in width and 50 mm in length were printed. Two different polymer compositions (PCL and a mixture of PCL and PEG), as well as two different drug loadings (50 % and 80 %) were tested. The percentage of total OLZ content released was 32.74 %, 59.34 % and 49.44 % for OP5, OPP5 and OPP8 implants, respectively.

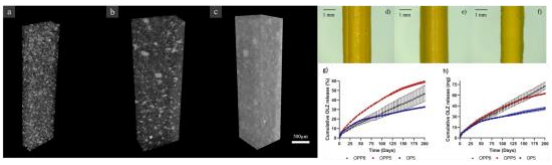

Figure 1. Maximum intensity projection µCT reconstructions of OP5 (a), OPP5 (b) and OPP8 (c). Images of the implants using the Leica E24W microscope at x16 magnification d) OP5, e) OPP5 and f) OPP8 implant.

DISCUSSION

The robocasting method proposed here possesses an additional advantage over conventional 3D-printing techniques, such as fused deposition modelling, as it does not require the use of high temperatures. Regarding the selection of polymers for implant fabrication, PCL was selected as it is both biocompatible and biodegradable and it has been used previously in the development of implants. The reduced overall drug release from OP5 compared to OPP5 could be attributed to the higher proportion of crystalline OLZ present within this formulation. Although OPP8 implants also contained PEG, they demonstrated reduced percentage drug release compared to OPP5 implants. Increased drug loading increases the crystalline proportion and, therefore, poorly soluble OLZ present in these implants. Nevertheless, the drug release profile of OPP8 implants is substantially more linear than the other implant formulations tested.

CONCLUSION

This work has demonstrated the usefulness of 3D-printing technology in the formulation of implants for long-acting delivery. Three different candidate implant formulations were successfully developed and manufactured. *In vitro* release studies demonstrated that all the formulations could maintain sustained drug release over a period of 200 days, with the maximum percentage drug release observed to be c.a. 60 % in the same period.

REFERENCES

Quarterman, J.C. *(et al.)*, Eur. J. Pharm. Biopharm. 159: 21-35, 2021.

Khaled, S.A. *(et al.)*, Int. J. Pharm. 461: 105-111, 2014.

MODULATION OF BACTERIAL INFECTION AND INFLAMMATION BY A LACTIDE-LOADED MATRIX SYSTEM

Kaifeng Huang, Louise Carson, Karl Malcolm, Matthew Wylie
School of Pharmacy, Queen's University Belfast
email: khuang07@qub.ac.uk

INTRODUCTION

Silicone elastomer is widely used for implant devices nowadays. However, bacterial infection caused by implantable devices made of elastomer is common[1]. DDU-4320, is a silicone elastomer can be used for vaginal rings. One of its drawbacks is its susceptibility to bacterial infection and can also give rise to inflammation[2]. Lactate is known to possess anti-inflammatory properties through activation of the GPR81 receptor, upon its hydrolysis to lactic acid in aqueous fluid, which can subsequently reduce inflammation[3]. Moreover, lactide is a ring polymer which is composed of a cyclic ester of two lactate molecules. In this study, lactide was loaded into silicone elastomer to exploit its biological effects which could be used in preventing bacterial infection and reducing inflammation.

METHODS

In this article, D, L-lactide was mixed with DDU-4320 and a matrix system made by injection molding. Lactide loading was investigated at three different loadings, which were 5%, 10% and 15% (w/w).

The amounts of lactide release and its degradation product, lactate, were quantified by reverse-phase HPLC with UV detection. Fibroblast cells were used to assess the cytotoxicity of the lactide-loaded elastomers. *Escherichia coli* and *Staphylococcus aureus* were used to assess the anti-bacterial efficacy of lactide upon release.

RESULTS

As Figure 1 shows, lactide release reached 100% within 5 days. In addition, when the percentage of loaded lactide was increased, the percentage of cumulative lactide released was elevated. Figure 2 shows the antibacterial efficacy of lactide-loaded elastomer systems when challenged with model Gram-positive and Gram-negative bacteria, *S. aureus* and *E. coli*, respectively. Antibacterial efficacy increased with higher loading of lactide, with 15% w/w-lactide systems capable of reducing viable bacterial adherence to <5% at 24 h. As a clear concentration-dependent effect was observed it is proposed that increased release of lactide from the silicone samples, and subsequent degradation to lactate, exerts either a broad-spectrum anti-adherent or an antimicrobial effect against bacterial cells.

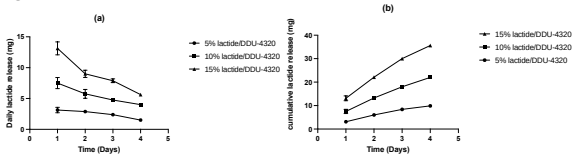

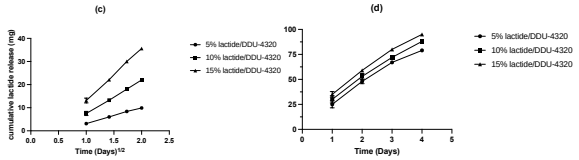

Figure 1. *(a) Daily lactide release. (b) Cumulative lactide release. (c) Cumulative lactide release (root time profile). (d) Percentage cumulative lactide release.*

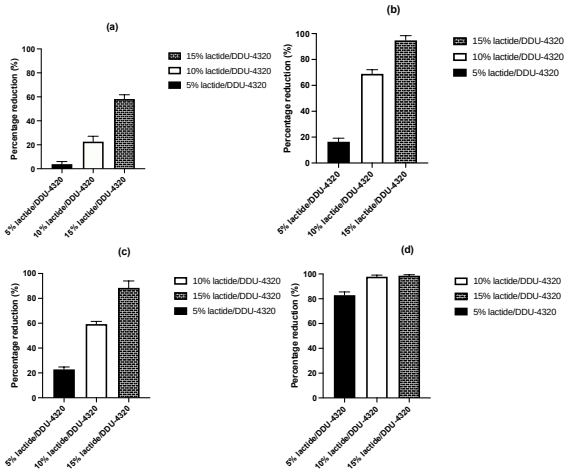

Figure 2. *Reduction in viable bacterial adherence, displayed as % reduction compared to unloaded control, after 4 h and 24 h incubations at 37ºC, for E. coli (a, b) and S. aureus (c, d).*

CONCLUSION

In conclusion, this study has found the incorporation of increasing loadings of lactide into silicone elastomer can reduce bacterial adhesion significantly, compared to control. This represents a non-antibiotic alternative strategy to prevent implant-associated infections. Future work will further elucidate the antibacterial mechanism of this strategy in preventing silicone surface colonisation and also assess the anti-inflammatory properties of lactide-loaded silicones.

REFERENCE

1. ZARE, M. (et al.), Journal of Applied Polymer Science, 138, 2021.
2. MURPHY, D. J. (et al.), J Control Release, 226**,** 138-47, 2016.
3. SUN, S. (et al.), Physiology (Bethesda), 32**,** 453-463, 2017.

PRODUCTION OF GEL PATCHES LOADED WITH ACYCLOVIR NANOCRYSTALS

Sangalli, M.[1], **Paredes, A.J.**[2]
[1] University of Pavia, Italy
[2] Queen's University Belfast, UK
(a.paredes@qub.ac.uk)

INTRODUCTION

Acyclovir (ACV) is an antiviral agent mostly used for the treatment of Herpes viruses, which possesses excellent activity towards the pharmacological target. However, due to its poor solubility and permeability, it needs to be administered multiple times daily to reach the therapeutic plasma concentration, resulting in side effects and lack of efficacy. The production of nanocrystals (NCs) is one of the most used approaches to improve the dissolution and absorption of hydrophobic and low permeability drugs. Among the production methods for drug NCs, wet media milling is one of the most preferred techniques due to its flexibility and ease for scale up. In order to avoid the costs related to the drying of the NCs such as the drug deposition on the walls of the drying machine, ACV aqueous nanosuspensions (NSs) were prepared and directly mixed with a hydrogel formulation, to produce dissolving gel patches loaded with ACV NCs.

MATERIALS AND METHODS

The formulation was milled for 24h and dynamic light scattering (DLS) was used to evaluate the particle size and polydispersity index (PDI) of the samples. The temperature, the number, the size and the position of magnetic stir bars were kept constant during all the experiments. In order to find the best formulation (lowest particle size and PDI), several nanosuspensions were prepared changing critical parameters in the formulation such as amount of ACV (50 mg, 100 mg, 150 mg); type and concentration of the stabiliser (P188, P407, SLS, Tween 80) - (0.25%, 0.5%, 1% w/v); rotation speed of the agitator (1100, 1200, 1300, 1500 rpm). The optimised NSs were mixed in a weight ratio of 1:1 with a gel formulation containing 50% water, 40% PVA and 10% glycerol. The gel patches were dissolved in Ultrapure water obtaining a concentration of 0.004 mg/mL and the physical stability of the NCs in the gels was determined using DLS. The drug content in the gels was evaluated by HPLC.

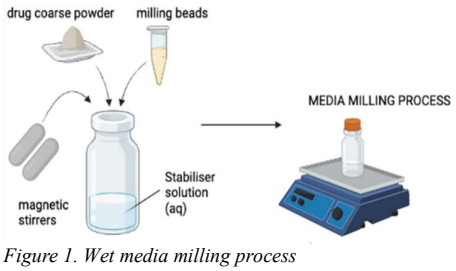

Figure 1. Wet media milling process

RESULTS

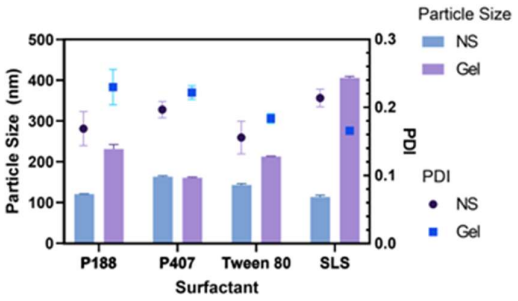

Figure 2. Comparison of the size of the NCs in the NSs and in the dissolved gel using different aqueous stabilisers [0.25%] w/v.

DISCUSSION

The parameters affecting the media milling process were thoroughly examined and modified while maintaining the same values for all other variables in order to achieve the smallest particle size. The most appropriate combination of factors for each trial was used to rationalise the process (100 mg of ACV, 5 mL of P407 0.25% w/v, 3.5 mL of beads, 1100 rpm). The optimisation of the media milling process revealed that all the stabilisers tested could be successfully used to prepare ACV NSs. Using SLS, the size of the NCs reached the smallest value of 114.47 ± 4.13 and a PDI of 0.215. The physical stability test conducted on the ACV gel patches showed that P407 is the only stabiliser tested which prevented physical aggregation of the NCs in the gel formulation. Indeed, the size of the NCs in the NSs and in the dispersed gel patch was respectively (163.40 ± 2.27, PDI 0.197; 161.24 ± 1.39, nm, PDI 0.222). The HPLC analysis showed that the patches prepared with P407 0.25% w/v achieved a drug recovery of 93-95 %.

CONCLUSION

The ACV media milling process was optimised, and a gel patch loaded with ACV NCs with a size of (161.24 ± 1.39) nm and a PDI of 0.222 was formulated. The patches containing 0.25% w/v of P407 showed an excellent drug recovery in the range of 93-95 %.

REFERENCES

O'Brien, J. J. "Campoli-Richards DM. Acyclovir. An updated review of its antiviral activity, pharmacokinetic properties and therapeutic efficacy." Drugs 37 (1989): 233-309.

McGucking, (et al), 2022. Nanocrystals as a master key to deliver hydrophobic drugs via multiple administration routes. Journal of Controlled Release, 334-353.

ROBUST ALGORITHM FOR DENSE SHAPE CORRESPONDENCE

Denton, O.[1], Hill, J.H[2]., Beverland, D.E[2]., Dunne, N.J. [3], Lennon, A.B[1]

[1] Queens University Belfast, School of Mechanical & Aerospace Engineering, Belfast, UK; [2]Musgrave Park Hospital, Primary Joint Unit, Belfast, UK; [3] School of Mechanical and Manufacturing Engineering, Dublin City University, Dublin, Ireland

email: odenton01@qub.ac.uk

INTRODUCTION

Statistical shape models (SSMs) are a method of parametrically defining variation between complex geometries. They allow instances of a geometry, beyond those in an observed training set, to be generated and are used in medical imaging, the design of patient-specific surgical tools and implants, inputs to FEA models, and phenotyping. Point-to-point correspondence between training geometries is a prerequisite for SSM building. However, many published techniques often fail to generalise across varied geometries. As a result, generating SSMs often requires specific domain knowledge, preventing application in several fields. Although automated workflows exist, these often implement a single Iterative closest point (ICP)correspondence algorithm. To address this problem, a correspondence algorithm that generalises between varied geometries was targeted, removing the required domain knowledge for model building.

MATERIALS AND METHODS

Modes of variation are synthetically generated about a single warping mesh, based on warping, translation, or rotation. These modes of variation are structured as deformation fields about the warping mesh, allowing them to be combined with an SSM where existing corresponding geometries are available. Each mode is defined by a point index, range, and magnitude defining the location and structure of the deformation. Different inputs lead to varied deformation behaviour. ICP or particle swarm optimisation (PSO) shape matchers match the shape model to a target shape. A further implementation of non-rigid ICP was applied sequentially, after matching the shape model, to minimise surface error. Correspondence was established between 3 warping meshes and 10 target meshes (30 total combinations) of both the pelvis and femur using coherent point drift (CPD) [1], optimal step non-rigid iterative closest point (OS-NRICP) [2], synthetic shape model fitting (SySM), and SySM followed by non-rigid ICP (SySM+). The root-mean-squared surface error (RMSE) and computation time were used for comparison.

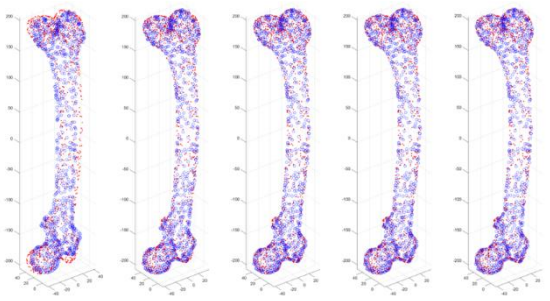

Figure 1 - the first 5 iterations of ICP matching between a Synthetic Shape Model and target mesh. The mean surface error dropped from 3.43mm prior to 0.49mm after matching.

RESULTS

Table 1 - Surface accuracy and computation time using CPD, OS-NRICP, SySM and SySM+. SI = Self-intersecting

		Femur			
		CPD	OS-NRICP	SySM	SySM+
RMSE (mm)	Warping 1	2.5	1.7	1.6	0.8
	Warping 2	2.8	1.5	1.3	0.4
	Warping 3	2.3	1.0	1.2	0.4
Time (s)	All	230	71	146	278
SI (%)	All	75	97	0	2
		Pelvis			
RMSE (mm)	Warping 1	3.0	1.1	1.2	0.3
	Warping 2	3.0	0.6	1.0	0.3
	Warping 3	2.3	1.5	1.3	0.4
Time (s)	All	222	73	134	237
SI (%)	All	60	97	0	0

DISCUSSION

A single correspondence workflow is shown to maintain a low surface error, whilst maintaining surface integrity (lack of mesh self-intersection) across varied geometries. This negates the need for parameter tuning based on geometry, warping mesh resolution and target mesh resolution. In doing so the requirement for domain knowledge is reduced. SySM+ has a computational time comparable to CPD but increased versus OS-NRICP and SySM, however, surface error is improved versus all compared methods. Whilst both SySM and SySM+ improve surface integrity versus CPD and OS-NRICP. In conclusion, a single correspondence workflow is shown to maintain surface accuracy in dense surface meshes of varied anatomic geometries. As part of a wider automated SSM building workflow, this facilitates SSM building without domain knowledge.

REFERENCES

[1] Myronenko (*et al.),* IEEE Transactions on Pattern Analysis and Machine Intelligence Vol 32 No 12, pg. 2262-2275, 2010

[2] Amberg *(et al.),* IEEE Computer Society Conference on Computer Vision and Pattern Recognition, Minneapolis, MN, USA, 2007.

CONJUGATION OF CATIONIC CELL PENETRATING PEPTIDE WITH NOVEL KUNITZIN-LIKE TRYPSIN INHIBITOR: NEW INSIGHTS FOR ENHANCING BIOACTIVITIES

Junting Yao[1], Lei Wang[2]
[1] School of Pharmacy, Queen's University Belfast, 97 Lisburn Road, Belfast, UK
email: jyao05@qub.ac.uk

INTRODUCTION

Cationic cell-penetrating peptides (CPPs) have been proposed as an effective drug carrier to improve intracellular delivery of biological macromolecules [1]. Amphibian skin-derived Kunitz-type trypsin inhibitors (KTIs), short counterparts of KTIs from plant sources, were widely found to possess potent serine protease inhibitory activity [2]. However, the poor transmembrane permeation capability of these molecules has largely hindered their biological activities [3]. CPPs were used to combine the natural peptides to enhance their bioactivities.

MATERIALS AND METHODS

Obtain the mature peptide sequence using molecular cloning method and bioinformatic analysis. Synthesis the peptides by solid phase peptide synthesis method. Purification and identification of peptides using RP-HPLC and MALDI-TOF. Trypsin and Chymotrypsin Inhibition determination. Antimicrobial screening by minimal inhibitory concentration (MIC) and minimal bactericidal concentration (MBC) assays. Anticancer screening by MTT cell antiproliferation assay. Cytotoxicity determination using haemolytic assay and LDH assay.

RESULTS

The peptide (Kunitzin-OV_2) and its phenylalanine-substituted analogue (F9-KOV) were evaluated for inhibition of trypsin/chymotrypsin and showed weak antibacterial activity against *Escherichia coli (E. coli)*. As expected, the conjugation did not increase membrane lysis compared to the parent peptide, but effectively assisted the parent peptide to enter the cell. TAT-KOV exhibited a 32-fold increase in antibacterial activity against *E. coli*. In addition, the conjugation enabled the parent peptides to exhibit anti-proliferative activity. Interestingly, TAT-F9-KOV showed stronger anti-proliferative activity against MCF-7 and U251MG cancer cells, which TAT-KOV did not have. Moreover, TAT-F9-KOV showed a 20-25-fold increase in anti-proliferative capacity against H157 and H460 cells compared to TAT-KOV.

```
   M  F  T  M  K  K  S  L  L  L  L  F  F  L  G  I  I
1ATGTTCACCA TGAAGAAATC CCTGTTACTC CTTTTTTTCC TTGGGATCAT

   S  L  S  L  C  K  E  E  R  D  A  N  E  E  R  R  D
51CTCCTTATCA CTCTGTAAGG AAGAGAGAGA TGCCAATGAA GAAAGAAGAG

   E  N  E  E  N  G  G  E  A  K  V  E  E  I  K  R
101ATGAAAATGA AGAAAATGGA GGGGAAGCTA AAGTGGAAGA AATAAAAAGA

   A  A  K  L  P  F  R  C  K  A  A  F  C  *
151GCTGCCAAAC TGCCTTTTAG GTGTAAAGCC GCATTCTGCT AAAACTAGAA

201TCAGTAAGGA TAATTGCTGT AATCAAAATA AAAATGTCAC ATACACCGTG

251GAAAAAAAAA AAAAAAAAAA
```

Figure 1. *Nucleotide sequence and corresponding translated amino acid sequence of kunitzin-OV_2 precursor cDNA. The putative signal and mature peptides are marked by double and single underlines, respectively. The stop codon is indicated by an asterisk.*

DISCUSSION

TAT was conjugated to the natural peptide in an attempt to increase the antibacterial activity and, as expected, TAT-KOV_2 and TAT-F9-KOV_2 exhibited a significant increase in antibacterial effect against *E. coli*, which was actually better than *S. aureus*. Previous studies showed that the surface of *E. coli* carries more negative charges than *S. aureus*, which is associated with negatively-charged lipopolysaccharides (LPS) on the outer protective membrane of this Gram-negative bacteria. Conjugation of cationic CPPs adds a large number of positive charges to the natural peptide complex, thus increasing its binding capacity to the LPS of Gram-negative bacteria

CONCLUSION

Kunitzin-OV2 is a novel peptide discovered from frog with trypsin inhibition and weak antibacterial ability. This is the first study of the conjugation of CPP with KTI. The results showed that conjugates formed by TAT with maternal peptides with different protease inhibitory functions did not produce cytotoxicity, while significantly elevating their antibacterial as well as anticancer abilities.

REFERENCES

1. Borrelli, A., et al., Cell Penetrating Peptides as Molecular Carriers for Anti-Cancer Agents. Molecules, 2018. 23(2): p. 295.
2. Chen, Y., et al., Structure-Activity Relationship and Molecular Docking of a Kunitz-Like Trypsin Inhibitor, Kunitzin-AH, from the Skin Secretion of Amolops hainanensis. Pharmaceutics, 2021. 13(7).
3. Dong, Y., et al., A Novel Kunitzin-Like Trypsin Inhibitor Isolated from Defensive Skin Secretion of Odorrana versabilis. Biomolecules, 2019. 9(7): p. 254.

AMOXICILLIN-LOADED PLCL ELECTROSPUN SCAFFOLDS FOR APPLICATIONS IN PERIODONTAL TISSUE ENGINEERING

Macartney, R.[1], Weaver, E.[2], Lamprou, DA.[2], Burke, GA.[1]
[1] Nanotechnology and Integrated Bioengineering Centre (NIBEC), School of Engineering, Ulster University
[2] School of Pharmacy, Queens University Belfast
email: macartney-r4@ulster.ac.uk

INTRODUCTION

Destructive periodontal diseases are the leading cause of damage to the supporting structures of teeth. This is the principal cause of tooth loss across the globe. Many of the soft tissues supporting the teeth themselves lack a high standard of regenerative capacity and therefore tissue engineered interventions are investigated to aid this process.

The use of biodegradable polymers has been frequently reported in the field of tissue engineering and regenerative medicine. Fabrication of scaffolds using the electrospinning technique reported here demonstrates production of scaffolds with geometry resembling closely that od the native extracellular matrix.

Early failure of implants is often caused by tissue integration issues. Lack of tissue integration is frequently owed to peri-implant infections, delayed wound healing and chronic inflammation. This is especially prevalent in terms of dental interventions due to the environment of diverse bacterial flora in the oral cavity. Therefore, here we investigate the addition of a broad-spectrum antibiotic during the electrospinning process as a preventative measure to reduce the potential for failed integration.

MATERIALS AND METHODS

Electrospun scaffolds encapsulating various concentrations of amoxicillin were produced using a medical grade polymer, Poly (D, L-lactide ε-caprolactone), PLCL.

Scaffolds were extensively characterised using physical, chemical, and mechanical analyses. Techniques applied include SEM imaging and associated image analysis, FTIR, Raman spectroscopy, and tensile testing methods.

Drug release from the electrospun scaffolds was investigated using high performance liquid chromatography. Cell viability/proliferation at the increasing concentrations of amoxicillin was investigated using an MTT assay.

RESULTS

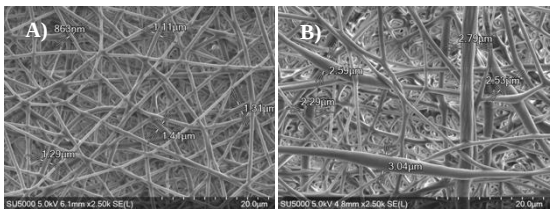

Figure 1 *SEM images showing the fibre morphology and measured diameters of* ***A)*** *0.5wt% amoxicillin and* ***B)*** *2wt% amoxicillin scaffolds.*

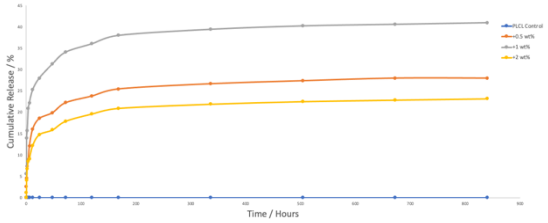

Figure 2 *Drug release profile showing release for control and amoxicillin loaded scaffolds.*

DISCUSSION

SEM analysis showed the encapsulation of amoxicillin within individual fibres throughout the matrix, demonstrating an increased fibre diameters after the addition of higher concentrations of amoxicillin during the electrospinning process. Increased intensity of Raman peaks validate the incorporation of amoxicillin to the fibre matrix. Mechanical analysis confirms that despite some alterations in properties following the addition of amoxicillin to the scaffold architecture, the scaffolds remain appropriate for tissue engineering of soft periodontal tissues.

The drug release profile describes a burst release, up to 72 hours of incubation. This was followed by a reduced rate of drug release which was sustained up to 35 days in the 1wt% amoxicillin samples. Investigations of *in vitro* cell viability via an MTT assay confirm that the incorporation of amoxicillin to the scaffolds does not have any cytotoxic effect up to 7 days of culture.

CONCLUSION

Scaffolds demonstrate appropriate properties for use in tissue engineering applications and *in vitro* studies demonstrate the potential for sustained drug delivery following implantation.

OSTEONECROSIS IN ORTHOPAEDIC DRILLING

Prasannavenkadesan, V.[1], Pandithevan, P.[2*]
[1]Queen's University Belfast, Northern Ireland, United Kingdom
[2]Indian Institute of Information Technology, Design and Manufacturing, Kancheepuram, Chennai, India
**email: (ppthevan@iiitdm.ac.in)*

INTRODUCTION

In surgical drilling, thermal osteonecrosis occurs when the temperature increases beyond 47 °C. Osteonecrosis is a major concern in orthopaedic surgery due to its adverse effects (implant loosening, misalignment of screw and plate), often leading to revision surgery. Factors contributing to the temperature rise in bone drilling are the apparent density, drill bit geometry, irrigation type and drilling parameters. This work aimed to assist the surgeons about how the temperature during surgical drilling influences the necrosis condition. Most of the works reported in literature were either simulation or experimental based. Very few studies were reported using statistical models. The proposed technique considers the probability density function that can help surgeons to distinguish between safe and risky regions in the femur to perform reconstruction surgery.

MATERIALS AND METHODS

A surgical drill bit of 3.0 mm diameter was used to make 4.0 mm deep holes in the cortical portion of the femur. The spindle speed of 1000 rpm and feed rate of 40 mm/min was used to mimic the manual surgical drilling procedure. A thermocouple was inserted in a pre-drilled hole (1 mm diameter with 2 mm depth) to record the temperature [1,2]. The femur bone used in this investigation was scanned, and reconstruction was performed by grouping CT data sets. Each group was constructed with eight slices, representing 0.5 mm slice thickness each. The method reported in the literature [3] was followed in this study to relate the CT number and apparent density. For the current investigation, 50 locations on the femur were selected, and the apparent density was computed. The goodness of fit was checked with the Kolmogorov-Smirnov test [4]. The critical test statistics was calculated at α=5%.

RESULTS AND DISCUSSION

The temperature generated during drilling in the longitudinal direction was recorded and fitted with the probability density functions. In the longitudinal direction, the test statistics for Weibull ($\widetilde{D}_{NW}$), lognormal ($\widetilde{D}_{Nl}$) and normal ($\widetilde{D}_{Nn}$) distribution were obtained as 9.69, 9.32 and 7.28, respectively. As $\widetilde{D}_{Nn} < \widetilde{D}_{Nl} < \widetilde{D}_{NW}$, the normal distribution ($\widetilde{D}_{\mathrm{Nn}} < \widetilde{D}_{\mathrm{N},\alpha}$) was considered for modelling when compared with the lognormal and Weibull three-parameter (3P) distribution.

Osteons are oriented along the drill bit axis when drilling in the longitudinal direction. Due to this, less force is sufficient for the drill bit to penetrate the bone. So, the in-situ temperature in the longitudinal direction drilling was lesser when compared with the drilling reported in other directions.

In earlier studies, it was observed that next to the longitudinal direction, drilling in the radial direction generated more temperature. With respect to drilling direction, the circumferential direction drilling was reported with higher temperature. Drilling through bone in the different regions with the same drilling parameters even with same apparent density resulted in different temperature. This may be due to the fact that the amount and orientation of pores vary with respect to the drilling direction.

CONCLUSION

The probability density functions were developed for the *in-situ* temperature recorded from bone drilling experiments. In this preliminary investigation, drilling through longitudinal direction is considered. As the models are direction based, the procedure reported in this work to be repeated for other directions even for same process parameters. The proposed methodology can assist the surgeon in selecting an optimal location for implant fixation using CT data sets as the only input. In future, it is aimed to adopt numerical simulation to investigate the thrust force and temperature during surgical drilling by considering the apparent density values and process parameters to reduce the experiments.

REFERENCES

1. Prasannavenkadesan *(et al.)*, Advances in Computational Methods in Manufacturing, Springer, 2019.
2. Prasannavenkadesan *(et al.)*, Proceedings of Institution of Mechanical Engineers Part E, 235:1984:1997, 2021.
3. Ciarelli *(et al.)*, Journal of Orthopaedic Research 9:674–682, 1991.
4. Yang *(et al.)*, Proceedings of Institution of Mechanical Engineers Part B, 218:1735:1740, 2004.

3D-PRINTED RESERVOIR-TYPE IMPLANTS FOR CURCUMIN DELIVERY

Korelidou, A. [1], **Dela Torre, A.**[1], **Kurnia Anjani, Q.**[1], **Domínguez-Robles, J.**[1], **Detamornrat, U.** [1], **Donnelly, R.F.** [1], **Larrañeta, E.** [1]

[1] School of Pharmacy, Queen's University Belfast, 97 Lisburn Road, Belfast BT9 7BL, UK
email: e.larraneta@qub.ac.uk

INTRODUCTION

Curcumin (Cur), the active constituent for turmeric is an anti-oxidant, anti-inflammatory, anticancer and anti-neoplastic molecule (Preetha et al.,2007). Cur restricting factors for the pharmacokinetic potential in clinical applications are its poor bioavailability due to its hydrophobic nature, poor stability and solubility (Preetha et al., 2007). Here we used three-dimensional (3D) printed biodegradable porous membrane implants developed by Fused Deposition Modelling (FDM) technology for local Cur delivery. In this study, we have increased Cur bioavailability by encapsulating it in a tablet, followed by the incorporation onto 3D printed implants. In this context, a Cur-loaded system was produced to cope with associated problems and to achieve controlled release kinetics.

MATERIALS AND METHODS

For tablet preparation, both components, excipient and Cur (purity 95 %) were mixed and placed into a dye (diameter 10 mm) which was placed into a manual hydraulic press (10 % w/w Cur in each tablet) as seen in Figure 1. Excipients used in this study for tablet preparation were: Soluplus®, 2-hydroxypropyl-β-cyclodextrin (HP-β-CD) and a combination of the above in 50:50 proportion (w/w %). Next, the tablet incorporated into a porous membraned implant that was prepared similarly to our previous work, with some modifications (Korelidou et al., 2022). For the *in vitro* release media, PBS (7.4 pH), a 0.5% w/v Tween® 80 was added, due to low Cur solubility in PBS.

RESULTS

Implants were prepared entrapping Cur tablets from either Soluplus®, HP-β-CD or their combination (Soluplus®+ HP-β-CD) (Figure 1). The combination of two different excipients incorporated for the preparation of Cur tablets, showed enhanced drug release. The release behavior showed a biphasic release pattern that previous studies of polymeric implantable devices have showed (Bansal et al., 2012). This release kinetics pattern is characterized by some initial burst release lasted for 7–9 days, followed by a slow controlled release. The three excipient formulations were released at different rates, with the cumulative mg release over 27 days being in the following descending order: Soluplus® + HP-β-CD (3 mg), HP-β-CD (0.6 mg) and Soluplus® (0.1 mg).

DISCUSSION

This burst release could be due to release of surface-bound drug and the excipient, followed by a more controlled release from the inner layers of implant's core. Addition of certain excipients in the tablet preparation can alter drug release significantly by changing the lipophilicity, porosity and the pH of the site (Weinberg et al., 2008). Such a burst effect as shown in the current work, can be desired in cases where rapid achievement of systemic concentration of therapeutic drugs is wanted and later be maintained with slow controlled release (Weinberg et al., 2008). Initial burst release delivers the drug for distribution to a large volume, to rapidly reach the therapeutic concentration and a slow, controlled release maintains the therapeutic concentrations for longer time (Weinberg et al., 2008). The current release showed a controlled drug delivery ability of Cur, after the burst release, which may lead to different behavior using different carrier system.

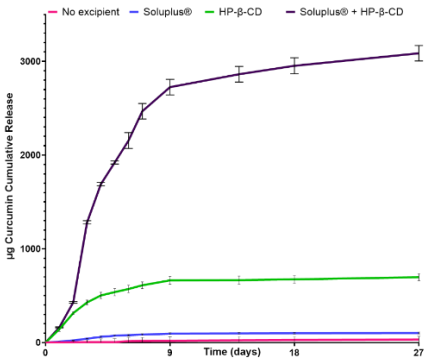

Figure 1. *In vitro* Cur release profiles from different mixing excipients over 27 days. Cumulative release in μg. Tablets without any excipient used as a negative reference (no excipient). Data points are expressed as means ± SEM, n = 4.

CONCLUSION

Implants, loaded with the proper choice of excipients and Cur could target a specific site of the body, protect the drug from degradation and deliver an even higher dose of the drug to the site of action, instead of distributing to other organs. This implant delivery concept could be applicable for many commonly used or yet not well studied therapeutic agents improving bioavailability issues that may have when administrated orally.

REFERENCES

Preetha et al., Molecular pharmaceutics. 4,6:807-18, 2007.
Korelidou et al., Biomaterials Advances. 139, 2022.
Bansal et al., European journal of pharmaceutics and biopharmaceutics. 80,3, 571-7, 2012.
Weinberg et al., Journal of pharmaceutical sciences. 97,5 1681-702, 2008.

REMOVAL OF VANCOMYCIN FROM WATER BY ADSORPTION USING WASTE MATERIALS

Abudu, L.S.[1], Rasoluli Sadabad, H[2], Adeyemi D.K[1], Oluseyi T[3], Adams L.A[3], Coleman H.M[4]
[1]Department of Pharmaceutical Chemistry, University of Lagos, Nigeria
[2]School of Geography and Environmental Sciences, Ulster University
[3]Department of Chemistry, University of Lagos, Nigeria
[4] School of Pharmacy and Pharmaceutical Science, Ulster University
Corresponding author email: h.coleman@ulster.ac.uk

BACKGROUND

The presence of antibiotics in the aquatic environment has posed huge challenges to human health globally with the generation of antibiotic-resistant bacteria . This has led to the spread of antibiotic resistance globally and caused about 1.27 million death in 2019 (Murray *et al.*, 2022).

These impacts are higher in developing countries like Nigeria, with a high rate of inappropriate use of antibiotics in addition to ineffective wastewater treatment plants (WWTPs) to remove these pollutants. (Akinyandenu et al, 2014; Ebele et al, 2020)

Lagos, a highly populated city in Nigeria is faced with challenges arising from poor management of solid municipal wastes from agricultural and food products such as banana stalks/skins and waste sawdust.

Previous studies have shown the potential use of lignocellulosic materials such as sawdust for the removal of antibiotics in water (Akinsanmi *et al.*, 2019). Vanocomycin has been listed by the WHO as a priority antibiotic due to it's resistance to known bacteria (WHO, 2019).

This study investigates the use of waste materials (sawdust from two sources) for the adsorption and removal of of vancomycin from water.

METHODS

The source of the sawdust was mahogany and tulip trees from Lagos, Nigeria. The sawdust was prepared by being washed, dried and blended into particles of sizes ranging from 46-460μm before undergoing pre-treatment with sulphuiric acid. For pre-treatment, 3g of the washed and dried sawdust was added to 100ml of 30% H_2SO_4 and shaken for 4 hours with the aid of an orbital shaker at 200 rpm. The sawdust was then placed in the oven at 60℃ for 2 hours and then washed and filtered using a Buchner funnel until a neutral pH was obtained. The untreated and treated sawdust was analysed for particle size distribution and polydispersity index. Adsorption experiments were conducted with vancomycin and monitored using HPLC with UV detection.

RESULTS

Particle size and the polydispersity index (PDI) of the untreated and treated sawdust are shown in Table 1. The result shows that there is a slight increase in the polydispersity index of both the sawdust from both the mahogany and the tulip treeafter treatment. The closeness of the PDI to 1 indicates the uniformity of the length of the chain of cellulose molecules in the sawdust and that this is much better in the treated sawdust.

There was an increase in the particle size for mahogany sawdusts and decrease in the tulip tree sawdust after treatment which would indicate a change in surface area and thus better adsorption for the vancomycin. Adsorption studies showed that both waste materials were effective for the adsorption of vancomycin in water and that the treated sawdust was more efficient.

Table 1: Particle size and polydispersity index of the treated and untreated sawdust samples from maghony and tulip trees

	Particle size (nm)	**Polydispersity index**
Untreated mahogany sawdust	3562	0.396
Treated mahogany sawdust	4899	0.859
Untreated tulip tree sawdust	6604	0.755
Treated tulip tree sawdust	2478	0.942

REFERENCES

Akinsanmi (*et al.*), 13th European wastewater managenment conference, Birminghan, United Kingdom, 2019

Akinyandenu (*et al.*), J sci Innov Res, 3(2): 251-257, 2014

Ebele (*et al.*), Emerging Contaminants 6: 124-132, 2020

Murray(*et al.*), The Lancet 399.10325: 629-655, 2022.

DUAL ACTION HYDROGEL COATINGS FOR THE PREVENTION OF URINARY CATHETER INFECTIONS AND BLOCKAGES

Burns, J.[1], McCoy, C.P.[1], Wylie, M.P[1], Irwin, N.J. [1]
[1] School of Pharmacy, Queen's University, Belfast BT9 7BL, United Kingdom
email: J.Burns@qub.ac.uk

INTRODUCTION

Catheter-associated urinary tract infections (CAUTIs) are challenging to treat due to device colonisation by uropathogens and encrustation. Encrustation occurs due to the presence of urease-producing bacteria, which can lead to catheter lumen blockage (1). Weak organic acids (WOAs) have been used as naturally occurring preservatives for centuries and exert their antimicrobial activity by the flow of unionised molecules through bacterial cell membranes, with subsequent reduction in intracellular pH, causing cell damage and death (1). WOAs have shown promising anti-encrustation and antimicrobial activity against uropathogens (2). Herein, the antibacterial activity of WOA-loaded hydrogel catheter coatings for the prevention of CAUTI is investigated.

MATERIALS AND METHODS

Formulations of ethylene glycol dimethacrylate (EGDMA), hydroxyethyl methacrylate (2-HEMA), polymethyl methacrylate (PMMA), polyvinylpyrrolidone (PVP), Irgacure® 2959 and citric/propionic acids were dip coated onto silicone sheets and all-silicone catheters at 200 mm min^{-1} before dried and cured with UVA light. Catheter bridge assays assessed *Proteus mirabilis* (*P. mirabilis*) ATCC 51286 swarming inhibition. Adherence and *in vitro* bladder model assays were performed for determination of *P. mirabilis* viability, urinary pH and time to catheter blockage.

RESULTS

Hydrogel coatings, (with and without WOAs), were observed to reduce viable *P. mirabilis* adherence by 94.27 - 99.99%, relative to uncoated silicone controls. However, hydrogel-coated catheter sections (with and without WOAs), were found to equally permit swarming of *P. mirablis (Figure 1)*.

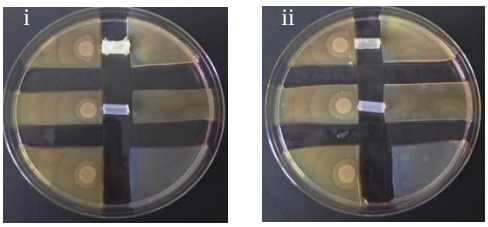

Figure 1: *P. mirablis swarming over 1 cm sections of coated and uncoated catheter bridges. Luria-Bertani agar plates with (i) WOA-loaded hydrogel coated catheters and, (ii) hydrogel coated catheters (without WOA), (n=3).*

In bladder models, the lumens of control catheters blocked within 46.38 h ± 3.16. Catheters with hydrogel coatings containing the citric/propionic acids combination displayed a small extension in time to blockage (53.51 h ± 13.12) indicating promising synergistic activity against uropathogens and encrustation *(Figure 2)*.

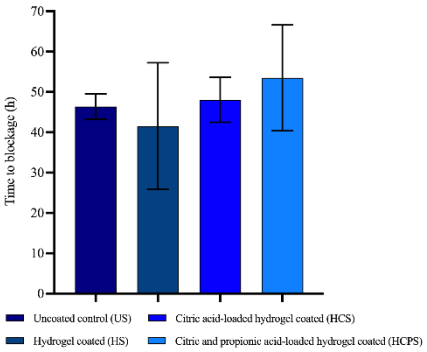

Figure 2: *Time taken for catheter blockage of uncoated and coated catheters when supplied with P. mirabilis-infected artificial urine ($1x10^9$ cfu mL^{-1}).*

DISCUSSION

Anti-adherent properties of the coatings may be dual action due to the antimicrobial and hydrophilic surface. Antimicrobial activity of WOAs is widely accepted to be pH dependent and an interfacial water layer on hydrophilic surfaces can act as a physical barrier to bacteria contact (2,3). However, hydrophilic hydrogel coatings have been shown to facilitate bacterial migration, as observed in the catheter bridge assay (4). Small extensions in time to blockage for catheters coated with hydrogel coatings containing the citric/propionic acids combination were due to the synergistic activity between the two compounds. Furthermore, acidic compounds have been found to reduce encrustation due to a reduction in urinary pH (2). However, release did not last for the lifetime of the device.

CONCLUSION

The dual action WOA-loaded hydrogel coatings present a promising new strategy for the prevention of CAUTI and catheter blockages. Future work will focus on extending the localised delivery of WOA.

REFERENCES

(1) Piper P *et al. Micro*. 147:2635-42, 2001.
(2) Burns J *et al. J. Hosp. Infect*. 111:69-77, 2021.
(3) Katsikogianni M *et al. Eu. Cells Mat*. 9:37-57, 2004.
(4) Sabbuba N *et al. BJU Intern*. 89:55-60, 2002.

Antibacterial Assessment of TMPyP-Incorporated p(HEMA-*co*-MMA)

Mahafdeh, Rania M.[1], Moore. Jessica V.[1], Wylie. Matthew P.[1], McCoy, Colin P.[1*]
[1] School of Pharmacy, Queen's University Belfast, Belfast, United Kingdom
[*]Corresponding author's email: (c.mccoy@qub.ac.uk)

INTRODUCTION

Light-triggered therapy to treat infectious diseases is called photodynamic antimicrobial therapy (PACT). PACT has been widely shown to have a lethal effect against bacteria, fungi, viruses, and parasites and it impacts different biofilms (Garcez et al., 2007) TMPyP (tetrakis(4-*N*-methylpyridyl)porphyrin) is a porphyrin frequently used in PACT, and exerts its phototoxic effect upon both gram-negative and gram-positive bacteria, via two reactions First, Type II reaction is considered the major pathway of photodynamic therapy. The second pathway, Type I reaction, involves transferring electrons/protons to a substrate and releasing a radical that can react with oxygen to produce reactive oxygen species (ROS) (Brady et al., 2007). This study aims to develop a novel surface loading with TMPyP capable of reducing the adherence of bacteria.

MATERIALS AND METHODS

TMPyP (tetrakis(4-*N*-methylpyridyl)porphyrin) IS the photosensitizer loaded into p(HEMA-*co*-MMA) hydrogel. *S. aureus* ATCC 29213 and *E. coli* ATCC 700928 which are required for the microbiological assessments. The LED light array activates TMPyP-incorporated p(HEMA-*co*-MMA). TMPyP was incorporated onto the surface of the p(HEMA-*co*-MMA) copolymer by swell-encapsulation shrink (SES) technique. Samples were prepared by loading them in different TMPyP soaking solutions for 2 min. First, a TMPyP stock solution was prepared (2.18 mg/ml). Next, further dilutions to the appropriate concentration were made using PBS (at pH 7.4). *S. aureus* ATCC 29213 and *E. coli* ATCC 700928 represent gram-positive and gram-negative bacteria and are used for assessing adherence percentages.

RESULTS

The percentage adherence (%) compared to dark control of *S. aureus* and *E. coli* when TMPyP-incorporated and unincorporated p(HEMA-*co*-MMA) were illuminated for 120 min using a white LED source providing a power of 5.33 mW/cm², integrated between 450–700 nm, or in dark condition has been presented in **Figure 1.**

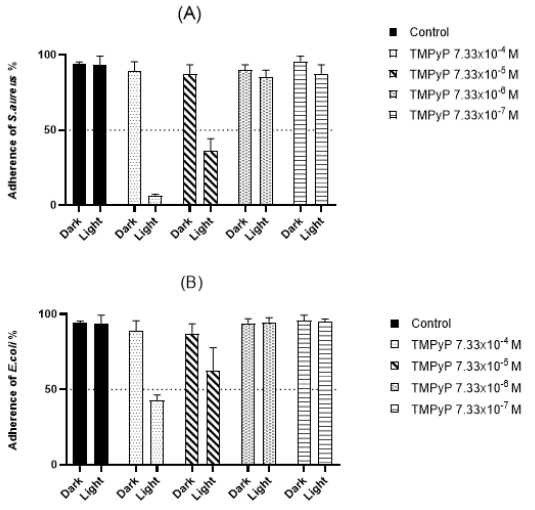

Figure 1. The percentage adherence (%) compared to dark control of (A) *S. aureus* and (B) *E. coli* Error bars represent ± S.D., n = 5.

DISCUSSION

TMPyP incorporated copolymers ($7.33x10^{-4}$ M and $7.33x10^{-5}$ M) significantly reduced the percentage adherence of *S. aureus* and *E. coli* compared to dark control illustrating that these materials are less likely to colonize. This antimicrobial behaviour for hydrogels loaded with $7.33x10^{-4}$ M of TMPyP shows significant promise for the development of biomaterials to prevent the colonization of gram-positive and gram-negative bacteria and prevent biofilm formation.

CONCLUSION

Overall, the attachment of TMPyP into the surface of p(HEMA-*co*-MMA) copolymers resulted in a material with antimicrobial behaviour.

REFERENCES

BRADY, C., BELL, S. E., PARSONS, C., GORMAN, S. P., JONES, D. S. & MCCOY, C. P. 2007. Novel porphyrin-incorporated hydrogels for photoactive intraocular lens biomaterials. *The Journal of Physical Chemistry B,* 111**,** 527-534

GARCEZ, A. S., RIBEIRO, M. S., TEGOS, G. P., NÚÑEZ, S. C., JORGE, A. O. & HAMBLIN, M. R. 2007. Antimicrobial photodynamic therapy combined with conventional endodontic treatment to eliminate root canal biofilm infection. *Lasers in Surgery and Medicine: The Official Journal of the American Society for Laser Medicine and Surgery,* 39**,** 59-66

Investigating the regenerative potential of 3D-printed PLLGA/Alginate composite scaffolds for the treatment of articular cartilage defects

Ghosh Dastidar, A.[1], A Clarke, S.[2], Buchanan, F.[1], Larranẽta, E.[3], J Kelly, D.[4], Rana, S.[4], Manda, K.[2]
[1] School of Mechanical and Aerospace Engineering, Queens University Belfast, Belfast BT9 5AG
[2] School of Nursing and Midwifery, Queens University Belfast BT9 7BL
[3] School of Pharmacy, Queens University Belfast BT9 7BL
[4] Trinity Biomedical Sciences Institute, Trinity College Dublin, Dublin D02 R590
email: aghoshdastidar01@qub.ac.uk

INTRODUCTION

Cartilage repair through bioresorbable scaffolds offers a promising alternative to current treatments, by providing cartilage regeneration and avoiding late-stage complications[1]. Commonly employed cell-encapsulated hydrogels offer limited success due to their insufficient biomechanical properties. To address this, 3d-printed Poly(L-Lactide-co-Glycolide) (PLLGA)/Alginate composite scaffolds have been fabricated and chondrogenic potential investigated with three cell types – goat mesenchymal stem cells (GBMSC), chondrocytes (GCH) and a co-culture (GBMSC:GCH) in a 42-day static culture. The composite scaffolds could respond to current unmet needs in a biomechanically comparable scaffold; increasing strength with a PLLGA matrix and promoting chondrogenesis using cell-encapsulated alginate. Zone-wise comparisons in scaffold (upper, middle, lower) were conducted to understand the effect of culture conditions.

MATERIALS AND METHODS

PLLGA 85:15 (purasorb PLG 8531) was 3d-printed using a bioscaffolder (Gesim, Germany) to a 6×6mm size by depositing a double-layer array of 10 layers. The cell types (GBMSCs, GCh, GBMSC:GCh) were mixed in alginate solution at a 1:1 ratio and cast in the pre-printed PLLGA scaffolds and crosslinked to form the composite. The chondrogenic potential was analysed using live/dead, histology, and biochemical assays over 42 days. Zone-wise comparisons (upper, middle, lower) were also conducted to understand the effect of culture conditions in a 3d-scaffold environment.

RESULTS AND DISCUSSION

The 3d-printed PLLGA matrix displayed interconnected pores (Fig. 1a&b) with minimal filament defects (Fig. 1c&d) containing the crosslinked alginate in the pores of the scaffold (fig. 1e). The compressive, equilibrium and dynamic moduli of these scaffolds were 1.05MPA, 1.74MPA, and 4.56MPA, respectively, that are biomechanically comparable to the native cartilage[4]. GBMSC, GCh and GBMSC:GCh embedded in the alginate showed high cell viability (>75%) and increased up to day 7 (fig. 1f). The groups displayed a strong cell population, composed of chondrocyte-like cells, in a fibrous matrix with a larger cell number from middle to the lower layers. The DNA quantification up to day 21 displayed stability in the GCh and GBMSC:GCh group indicating a cartilage-like behavior where cells do not proliferate. GBMSC on the other hand showed a decrease in cell number over 21 days potentially due to the hypoxic conditions experienced in the scaffold core. An increased sGAG production in the GBMSC:GCh group displays stronger chondrogenic potential in the co-culture group, however the collagen production is similar in 21 days in all the groups. Further studies on histological staining are currently in progress. Biomechanical stimulation has been widely studied on primary cell culture groups to understand its effect in a 3D scaffold environment. However, to compare this with a co-culture group would be a valuable insight into its future translation as a medical device. It has been hypothesized that the co-culture group would enhance cartilage regeneration better than the other cell groups in the composite scaffold.

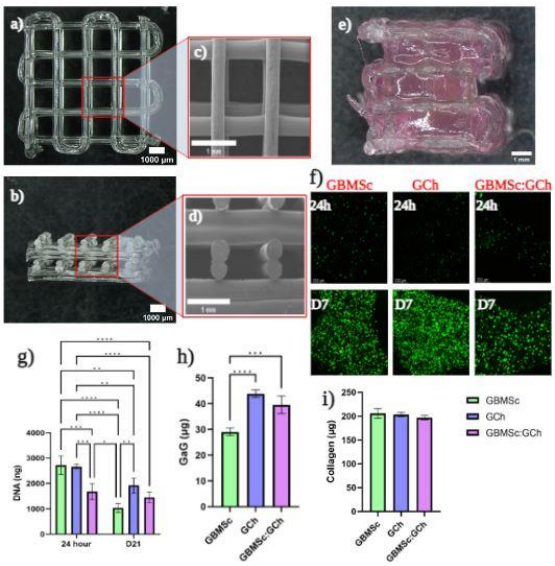

Figure 1(a) 3D-printed PLLGA scaffold (b)cross-sectional image (c) SEM image of the scaffold (e) SEM image of the cross-section (e)composite scaffold (f) Live/dead assay (g) DNA (h) sGAG (i) Total collagen quantification n = 4, ⁎significance, $p < 0.05$

CONCLUSION

These results show that pllga/alginate composites balance the requirement for scaffold material with robust mechanical properties, and strong biocompatibility and chondrogenesis across cell types, demonstrating the potential for cartilage tissue regeneration.

REFERENCES

[1]Mobasheri et al., Ost&Cart Open. 3;100146(2021). [2]Geddes et al., Pol.Testing. 91;106853(2020). [3]Guo et al., Biofab. 9;(2017). [4]Mansour., Kinesiology.66-79 (2003).

ACKNOWLEDGEMENTS

This project has received funding from the engineering and physical sciences research council under a PhD studentship.

REPLICATION OF POLYMERIC BIROESORBABLE VASCULAR SCAFFOLD PROCESSING HISTORY WITH FOCUS ON CRIMPING

Barr, J.[1], Menary, G.[1], Lennon, A[1].
[1]School of Mechanical and Aerospace Engineering, Queen's University, Belfast, UK
email: (jbarr20@qub.ac.uk)

INTRODUCTION

The potential of polymeric bioresorbable vascular scaffolds (BVSs) present a promising alternative to permanent metallic stents to treat coronary heart disease, providing key issues can be overcome. Their reduced mechanical properties mean they require thicker struts, which have been linked to poor deliverability, injury to the vessels, and deposition of platelets (which can cause thrombus formation) [1]. Understanding and tailoring the processing steps may be key to designing an improved, fit for purpose, BVS. Significant localised deformation occurs during the crimping and deployment phases and may be important for optimising spatial distribution of material morphology [2,3]. This work aims to investigate the influence of crimping and deployment on final BVS properties by idealising the processing history through controlled experiments that mimic each stage of the manufacturing process.

MATERIALS AND METHODS

PLLA, PURASORB PL38 (Corbion, Netherlands) was extruded into 1 mm thick sheet. The tube expansion process was emulated through biaxial stretching. A design of experiments (DOE) programme was employed to investigate extremes of stretching parameters; temperature (79-86°C), stretch ratio (2-2.75), strain rate (4-16s^{-1}) and process (simultaneous-sequential). Tensile tests at 5mm/min were carried out to determine mechanical properties of the stretched sheets. U-bend specimens were laser cut from stretched sheets produced with varying stretch ratio as the critical factor. With particular focus on crimping, high and low values for crimp duration (6-600s) and temperature (21-50°C) were selected. U-bend specimens were then tested in a custom-rig [4] using combinations of these conditions to compare force-displacement responses (Figure 1a). SEM imaging was also used to assess deformation and damage, if any, occurring during testing. Alongside physical experiments, the mechanical data collected from tensile testing (Figure 1c) was used to fit elastic-plastic material models to enable FEA of the crimping tests in ABAQUS (Dassault Systèmes Simulia Corp, USA).

RESULTS AND DISCUSSION

Main effects plots from DOE (Figure 1d) show that stretch ratio is the dominant factor for modulus. Both modulus and yield strength are highest when tensile test specimens were cut in the sheet's dominant stretch direction, while ductility is highest when the opposite is true. Load displacement graphs clearly show different mechanical responses of the U-bend specimens during different crimping conditions. This data is also comparable with FEA predictions; however, differences occur during the plastic portion of deformation. Further work is being undertaken to incorporate rate-dependent effects, which are not captured by the initial elastoplastic material model. SEM images confirmed expected deformation occurring during crimping relative to FEA predictions and literature (Fig. 1b) and have identified cases when damage, in particular cracks, has caused a larger than expected drop off in load. Analytical stress-strain analysis based on curved beam bending is being developed to allow consistent comparison between specimens of different thickness and to refine validation from the FE model.

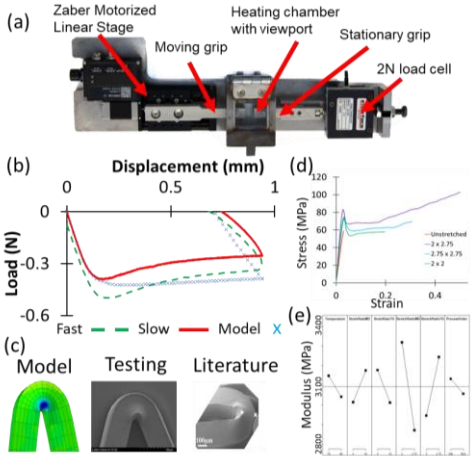

Figure 1: (a)Crimp Test Rig. (b) Representative crimping test results comparing fast, slow and model data. (c) images showing deformation that occurred in modelling, testing and literature [3]. (d) Tensile stress-strain graphs of unstretched and stretched sheets used for U-bend specimens. (e) Modulus main effects plot from DOE.

A key benefit of the idealised design when compared with conventional crimping methods is that it enables unique characterisation techniques, such as x-ray scattering and DIC, during deformation which could not previously be achieved. Results of the U-bend crimp tests have shown the importance of ductility, with heating (to some extent), able to overcome brittle cracking in less ductile specimens. Replicating the processing history of BVS in an idealised way provides a new framework for analysing BVS processing parameters on BVS-relevant structural features.

References
1. Ang (et al.), Journal of Thoracic Disease, 9:923-934, 2017 2. Wang et al., PNAS 115:2640-2645, 2018 3. Ramachandran et al., PNAS 115:10239–10244, 2018 4. Barr et al, BinI 27, 62, 2022

ADVANCING SURGICAL CARE: BIACTIVE GLASS SYSTEM FOR TARGETED ANTIBIOTIC DELIVERY IN PREVENTION AND TREATMENT OF SURGICAL SITE INFECTIONS

Humera, Sarwar.[1], Coleman, Heather [1], Courtenay, A.J [1], Deborah, Lowry *[1]

[1] *Ulster University, School of Pharmacy and Pharmaceutical Sciences, BT52 1SA, Coleraine, Northern

email: (d.lowry@ulster.ac.uk)

INTRODUCTION

Antimicrobial resistance (AMR) has become a growing concern in healthcare, posing significant challenges in treating and preventing surgical site infections (SSIs) [1]. Limited treatment options, an increased risk of SSIs, reduced effectiveness of prophylactic antibiotics, and inadequate infection control measures are some of the difficulties posed by AMR. Biomaterials, such as bioactive glass, have shown great potential in preventing and treating SSIs through various mechanisms, such as providing a physical barrier against bacteria, releasing antimicrobial agents, or promoting tissue healing. Bioactive glass is a unique type of glass that can interact with biological tissues, promoting tissue regeneration and preventing bacterial adhesion and biofilm formation [2]. This property makes bioactive glass an attractive material for use in medical devices, including drug delivery systems. Recent studies have shown that bioactive glass-based delivery systems for targeted antibiotic delivery are effective in preventing and treating SSIs. The combination of bioactive glass with antibiotics is an area of active research, and it has potential benefits for the treatment of infections arising during bone repair and surgeries [5].

MATERIALS AND METHODS

Bioglass cores, including 45s5 and 45s5 3% Gallium, were coated with trehalose and sucrose at ratios of 1:1, 1:2, and 1:3. The resulting mixture was stirred, centrifuged, and washed with PBS buffer. The coated particles were collected, lyophilized, and loaded with 0.5% w/v Vancomycin HCl. The particles were then analysed for loading efficiency, size distribution, and zeta potential. In vitro drug release was carried out using a dialysis tubing method for 168 hours, and the samples were analysed on a UV-Vis spectrophotometer at 280 nm. Antimicrobial characteristics were analysed using the zone of inhibition assays.

RESULTS

The majority of the formulation size distribution was observed to be approximately 500 d.nm. A decrease in the polydispersity index (PDI) was observed after the loading of vancomycin, which may be attributed to the reduction in surface tension of ceramic nanoparticles due to the addition of drug up to a certain concentration. The f4l formulation exhibited model-dependent release (Makoid Banakar), indicating that the drug release followed four parameters of release, including initial burst release, lag time, release rate, and duration of release.

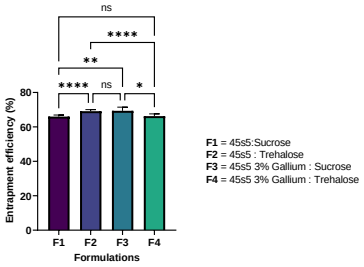

Figure 1 Loading efficiency.

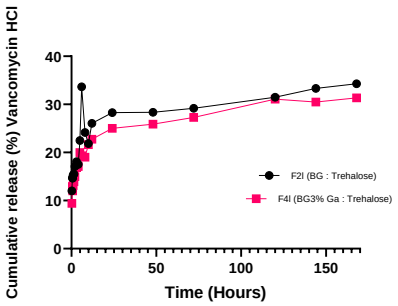

Figure 2 Cumulative release of Vancomycin HCL loaded Bioglass45s5 and Bioglass 45s5 3% Gallium

CONCLUSION

In conclusion, Bioglass demonstrates unique properties that make it a promising biomaterial for the prevention and treatment of infections. In the current study, Bioglass was utilized as a core for antibiotic delivery, exhibiting controlled release for up to 7 days and potentially longer. Further investigation is underway to analyse the in vitro kinetic parameters and characterize the synthesized formulations.

REFERENCES

1. Allegranzi B, et al. Lancet Infect Dis. 2016;16(12): e276-e287.
2. Hench LL, et al. J Biomed Mater Res. 1973;7(3):25-42.
3. Hasan J, et al. Trends Biotechnol. 2013;31(5):295-304

DETERMINING ACTIVE DRAG IN SWIMMING VIA COMPUTATIONAL AND EXPERIMENTAL MEANS

Haskins, A.[1], Lennon, A.[1], Chandar, D.[1] Geron, M.[1]
[1] School of Mechanical and Aerospace Engineering, Queen's University Belfast
email: ahaskins02@qub.ac.uk

INTRODUCTION

Active drag in swimming is the resistance force that acts on a swimmer whilst swimming and is constantly changing across a stroke cycle [1]. To investigate the drag associated with an athlete's technique, active drag must be found via experimental or computational means. Current methods of experimental active drag prediction tend to see a high level of interference with the athlete's technique, such as the MAD system [2]. Current methods are also unable to predict how the active drag of an athlete's technique vary across a stroke cycle, instead assuming an average value of active drag acting across the full stroke cycle.

The method outlined below aims to provide an active drag profile over a full Freestyle stroke cycle. These results will be used to validate CFD results, determined using the finite volume immersed boundary method.

MATERIALS AND METHODS

An experiment was conducted using 7 elite level male athletes. Each athlete repeated each sub-experiment twice, resulting in 14 data sets. Two sub-experiments were completed: one using a fully tethered load cell setup, allowing the propulsive force *excluding* the drag to be found across the stroke cycle, and one using a 1080 Sprint resistance trainer, allowing the propulsive force *including* the drag to be found across the stroke cycle. The active drag at each corresponding stroke position was then calculated as follows:

$$A_d = PF_{nd} - PF_d \quad (1)$$

Where A_d is active drag, PF_{nd} is propulsive force *excluding* drag and PF_d is propulsive force *including* the drag. Following this, a steady state CFD simulation was completed, using OpenFoam, for results comparison.

RESULTS

Figure 1 displays the results of the average and standard deviations of active drag across the 14 trials.

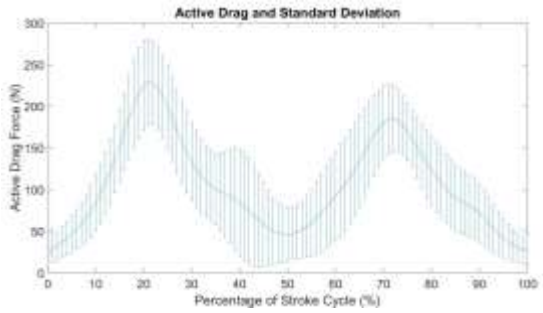

Figure 1: Average active drag profile of 14 trials

Results ranged between approx.. 0-50 N and 150-350 N across the stroke cycle. Each stroke cycle was split into percentages to clearly display when in the stroke each value of drag occurs. The CFD results showed a drag value of 120 N at a velocity of 2 ms^{-1}, with a streamline plot of the 0% position of the model visible in Figure 2.

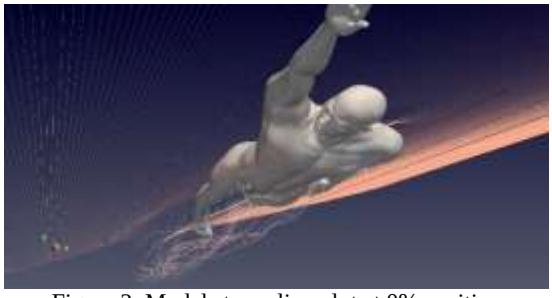

Figure 2: Model streamline plot at 0% position

DISCUSSION

The experimental results are comparable in magnitude with Mason [3] (average active drag across the stroke cycle of 112–253 N, and Toussaint [4], (127–169 N. The CFD drag of 120 N for the 0% position is similar in magnitude to the experimental results for the 0% position, shown in Figure 1. Although the experiment found a value of between 0-50N, this difference is likely caused by the unsteady nature of the real swimming compared to a steady state CFD simulation. Other reasons for the difference are due to the average velocity of swimming in the experimental section being lower than the velocity used during the CFD. Unsteady CFD simulations for each technical position percentage point would be required for accurate comparison of results.

The novel active drag measurement provides a good estimation of the active drag experienced by an athlete, when compared to CFD and existing experimental methods. The method is also able to provide a profile of how the drag changes across the stroke cycle. Improvements to the method could be made by using a synchronised camera to aid stroke identification and stroke cycle position. More trials per athlete could be used to provide a more accurate representation of the athlete's average active drag profile.

REFERENCES

1. Voronstov, A. R et al, *Biomechanics in Sport*, 2008
2..Hollander, A. P et al., *J. of Sports Sciences*, 1986.
3.Mason, B et al, *Portuguese J. of Sport Sciences*, 2011.
4.Toussaint, H. M et al, *J. Biomech.*, (1988).

SYNTHESIS AND CHARACTERISATION OF SILVER NANOPARTICLES AS A COMPONENT OF ANTIBACTERIAL HYDROGEL COATINGS IN PERIODONTAL DISEASE DIAGNOSTICS

Mensah, A.[1], Courtenay, A.J.[1]*

[1]*Ulster University, School of Pharmacy and Pharmaceutical Sciences, BT52 1SA, Coleraine, Northern Ireland, United Kingdom

email: (a.courtenay@ulster.ac.uk)

INTRODUCTION

The antibacterial properties of silver nanoparticles are well-documented and have been extensively researched for various biomedical applications.

There is a growing interest in the use of silver nanoparticles and hydrogels for biomedical applications such as wound healing. Silver nanoparticles and hydrogels have low toxicity levels in the body, increasing their safety for use in biomedical applications (1,2). In periodontal disease, researchers have investigated the use of silver nanoparticles and hydrogels as a promising approach for periodontal disease treatment. Studies have shown that silver nanoparticles and hydrogels can effectively inhibit the growth of periodontal pathogens, reduce inflammation, and promote tissue regeneration (3). The method of synthesis of silver nanoparticles is crucial for ensuring the efficacy and reliability of antibacterial properties (2, 3). This work therefore seeks to evaluate the optimum protocol for the synthesis of synthesis of silver nanoparticles to be incorporated into hydrogels as coating material in periodontal disease diagnostics.

MATERIALS AND METHODS

Eight silver nanoparticle formulations were made and coded from AF1-4 and BF1-4.

The method used in this study involved the reduction of silver ions using sodium borohydride as a reducing agent in a ratio 20:1 by volume.

Polyvinyl alcohol and starch were used as stabilizing agents at concentrations of 0.3%w/v,4%w/v for PVA and 0.2%w/v,0.5%w/v for starch. The concentrations of the stabilizing agents were with respect to the volume of $AgNO_3$.

The formulations were characterised with dynamic light scattering (DLS) and UV-visible spectroscopy. These techniques allowed for the determination of particle size, particle size distribution as well as the confirmation of silver content. The effect of the stabilizing agents and concentration of the $AgNO_3$ solution on the parameters listed above was also investigated.

RESULTS AND DISCUSSION

The silver nanoparticles had an average size range between 47 and 2781 nm and a size distribution from 0.246 to 1.000 (Table 1). All formulations showed a single peak at wavelength of 399.9 nm. There was a trend of increased absorbance of formulations with increasing concentration of $AgNO_3$ and of the AgNP is proportional to the concentration of the starting silver solution. PVA stabilised AgNP solutions produced higher UV-vis absorbance compared with starch stabilised solution (Figure 1).

Table 1: Mean diameter of particles and polydispersity index of nanoparticle formulations. (n=3 ± SD)

Parameters	0.001M $AgNO_3$				0.005M $AgNO_3$			
	AF1	AF2	AF3	AF4	BF1	BF2	BF3	BF4
Mean diameter of particles (nm)	87.62 ± 1.19	48.86 ± 1.25	88.46± 1.30	939.90 ± 22.89	91.26± 1.07	47.05 ± 0.43	123.20± 6.61	2781.00± 114.90
Polydispersity index (PDI)	0.38 ± 0.05	0.39 ± 0.01	0.29± 0.01	0.25± 0.02	0.39 ± 0.004	0.44± 0.004	0.60 ± 0.10	1.00 ± 0.00

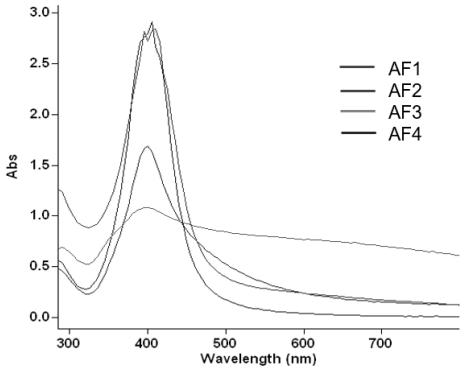

Figure 1: UV-vis spectra of AgNP fabricated with 0.001M $AgNO_3$ and 0.002M $NaBH_4$ with varied concentrations of stabilizing agent.

CONCLUSION

We have demonstrated that the method of reduction of Ag+ to Ag by sodium borohydride as the reducing agent and PVA as the stability agent produced uniform silver nanoparticles with characteristics that can allow successful incorporation into hydrogels.

REFERENCES

1. Zhang *et al., International journal of molecular sciences, 17(9), 1534, 2016.*
2. *Wang et al., Advanced Composites and Hybrid Materials, 4, 696-706, 2021.*
3. *Shen et al., ACS Sustainable Chemistry & Engineering, 8(19),7480-7488, 2020.*